

## 2. Theoretical Background, Results, and Discussion

### 2.1 Octahedral versus Trigonal prismatic conformation

G. Wilkinson and A. Shortland reported very briefly in 1972 on the synthesis of the new complex hexamethyl tungsten.<sup>[4a]</sup> One year later both authors were able to characterize this compound and reported that  $W(CH_3)_6$  was octahedral: “the i.r spectrum is consistent with an octahedral structure”.<sup>[4b]</sup> Furthermore in 1975 Wilkinson and Galyer recorded the photoelectron spectra of hexamethyl tungsten and concluded that: “the photoelectron spectra of hexamethyl tungsten is consistent with octahedral symmetry”.<sup>[4c]</sup> The first theoretical calculations (1986) for certain  $d^0$  complexes predicted a non octahedral structure as the conformation with the minimum energy.<sup>[1]</sup> In 1989 P. Morse and G. Girolami found that the crystal structure from the anion  $[Zr(CH_3)_6]^{2-}$  was an almost regular trigonal prism,<sup>[2]</sup> and one year later A. Haaland et. al. proved from the gas-phase electron diffraction study on  $W(CH_3)_6$  that it possess a trigonal prismatic coordination geometry,<sup>[5]</sup> after which many theoretical investigations concerning these findings were undertaken.<sup>[7-11]</sup>

Finally this controversy was resolved in 1996 when V. Pfennig and K. Seppelt elucidated the structures of the first two examples of a neutral, non octahedral, hexa-coordinated homoleptic complexes  $W(CH_3)_6$  and  $Re(CH_3)_6$ .<sup>[6]</sup> This marked the beginning of the interesting chemistry about the possible octahedral versus trigonal prismatic conformation of six coordinated complexes.

In the past few years, the number of neutral complexes  $[Mo(CH_3)_6]$ ,<sup>[15]</sup>  $[(CH_3)_5MoOCH_3]$ ,<sup>[16]</sup>  $[(CH_3)_4Mo(OCH_3)_2]$ ,<sup>[16]</sup>  $[(CH_3)_5WCl]$ ,<sup>[16]</sup>  $[(CH_3)_3WCl(OCH_3)_2]$ ,<sup>[16]</sup>  $[(CH_3)_5MoOCH_3]$ ,<sup>[16]</sup> and anions  $[(Nb(CH_3)_6)]^-$ ,<sup>[17]</sup>  $[Ta(CH_3)_6]^-$ ,<sup>[17]</sup>  $[Ta(C_6H_5)_6]^-$ ,<sup>[18]</sup>  $[Ta(C_6H_4-4-CH_3)_6]^-$ ,<sup>[18]</sup> having a trigonal prismatic structure (distorted in some cases) has increased remarkably. Ab initio and DFT calculations<sup>[12,13]</sup> on such species also reveal a trigonal prismatic structure as the conformation with the minimum energy requirements.

What are the mechanisms that interconvert an octahedron into a trigonal prism? The first publication dealing with a possible mechanism for the octahedral versus trigonal prismatic rearrangement appeared in 1943.<sup>[21]</sup> In 1953, based on a series of studies in optically active hexa-coordinated complexes, J. C. Bailar Jr. proposed a mechanism which is known as the Bailar twist.<sup>[19]</sup> On a later publication C. S Springer and R. Slevers said that “the Rây-Dutt twist from 1943 is a special case of the Bailar twist about an imaginary  $C_3$  axis” and concluded that “the Bailar twist proved to be a very general intramolecular non-bond rupture mechanism which can account for both optical and geometrical isomerization of octahedral complexes”.<sup>[22]</sup> Based on a mathematical analysis which is beyond the scope of this work, Klemperer<sup>[20]</sup> postulates 6 “distinguishable permutational isomerization reactions” for a six coordinate octahedral molecule see figure 1.<sup>[20]</sup>

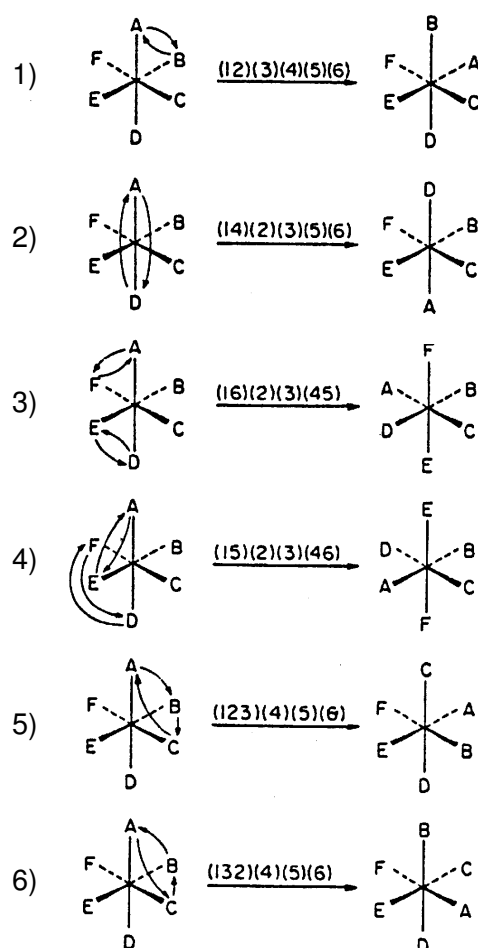


**Figure 1.** Six differentiable permutational isomerization reactions of a six coordinate octahedral molecule in a **chiral** environment (taken from ref. [20]).

In figure 1 the numbers in parenthesis indicate permutations of the positions which are denoted by letters (A to F) in each molecule. In a totally symmetric environment, reaction schemes 1, 2, and 5 (from top to bottom) are the only differentiable permutational isomerization reactions. Reaction schemes 5 and 6 correspond to the Bailar twist mentioned before and reaction scheme 1 is the one responsible for the permutation of *cis* ligands, which Hoffman, et. al. used to explain the so called bicapped tetrahedron structure obtained from an octahedron which has been seen in some  $H_2ML_4$  dihydrides.<sup>[14]</sup>

In a very recent publication D. Casanova, et. al.<sup>[23]</sup> studied the possibility of interconverting an octahedron into a trigonal prism and vice versa based on what they call “the minimal distortion pathway” and proved this theory using experimental evidence based on more than 300 complexes which are either octahedral or trigonal prismatic. The authors formulated the mathematical expression for a curve which provides the distortion of an octahedron into a trigonal prism (or vice versa) and at the same time produces the minimum distortion of the shape. Experimental structures are compared to this “minimal distortion pathway” and are found to fit extremely well. They concluded that from all possible octahedral and trigonal prismatic structures that they studied all lie in this minimal distortion pathway and that “this mathematical expression is fully consistent with the Bailar twist for hexa-coordinated complexes”.<sup>[23]</sup>

What exactly is the Bailar twist? In figure 2.a, an octahedral species is rotated  $60^\circ$  through one of the  $C_3$  axes of the molecule producing a trigonal prismatic structure. If this triangular face of the trigonal prismatic structure is rotated once more  $60^\circ$  the end result would be an octahedron in which three positions have been changed (namely (123)(4)(5)(6) to (312)(4)(5)(6) as an example). Figure 2.b shows a special case of the distortion proposed by Hoffman, et. al.,<sup>[14]</sup> which produces also an octahedral-trigonal prismatic rearrangement. If two adjacent ligands of an octahedron are rotated  $45^\circ$  and then all other angles rearranged themselves a trigonal prismatic structure is obtained. If the rotation is completed to  $90^\circ$  a bicapped tetrahedral structure is obtained.<sup>[14]</sup>

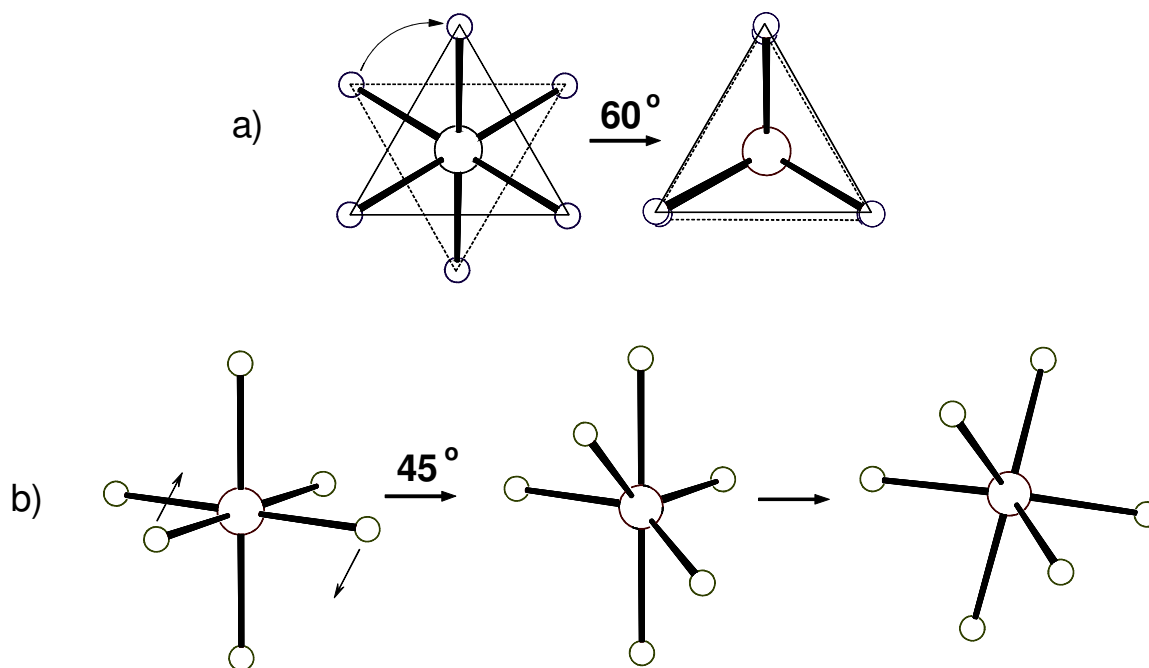


**Figure 2.** a) Bailar twist, also called 3+3 (or 3:3) rearrangement, b) 2+4 (or 2:4) rearrangement for octahedral-trigonal prismatic structures.

What are the conditions that need to be fulfilled for a trigonal prismatic structure to prevail over the octahedron for the metal complexes? Hoffman, et. al.<sup>[14]</sup> concluded that the geometry of a particular complex is not only governed by the d orbital patterns but also by the various structural parameters of the coordination sphere (size of the metal ion, steric interference of the ligands) and that:

1. Low numbers of d electrons ( $d^0$  and  $d^2$  metals) are the optimum situation for trigonal prismatic coordination.
2. For a given d electron configuration the lower the energy of the metal d orbitals, the stronger the metal-ligand bonding in the trigonal prism (there is a better  $\sigma$  bonding situation).

S. Kang, T. A. Albright, and O. Eisenstein<sup>[7]</sup> concluded that even though  $C_{3v}$  and  $D_{3h}$  geometries are sterically much more demanding than  $O_h$ :

1. For obvious steric reasons the ligands must not be bulky.

2. The  $t_{2g}$ - $t_{1u}$  energy gap (see figure 3<sup>[9]</sup>) should be small which is favored when the ligands are strong  $\sigma$  donors, possess little or no  $\pi$ -donating capability, and the metal is not too electropositive.

3. The metal-ligand bond should be largely covalent.

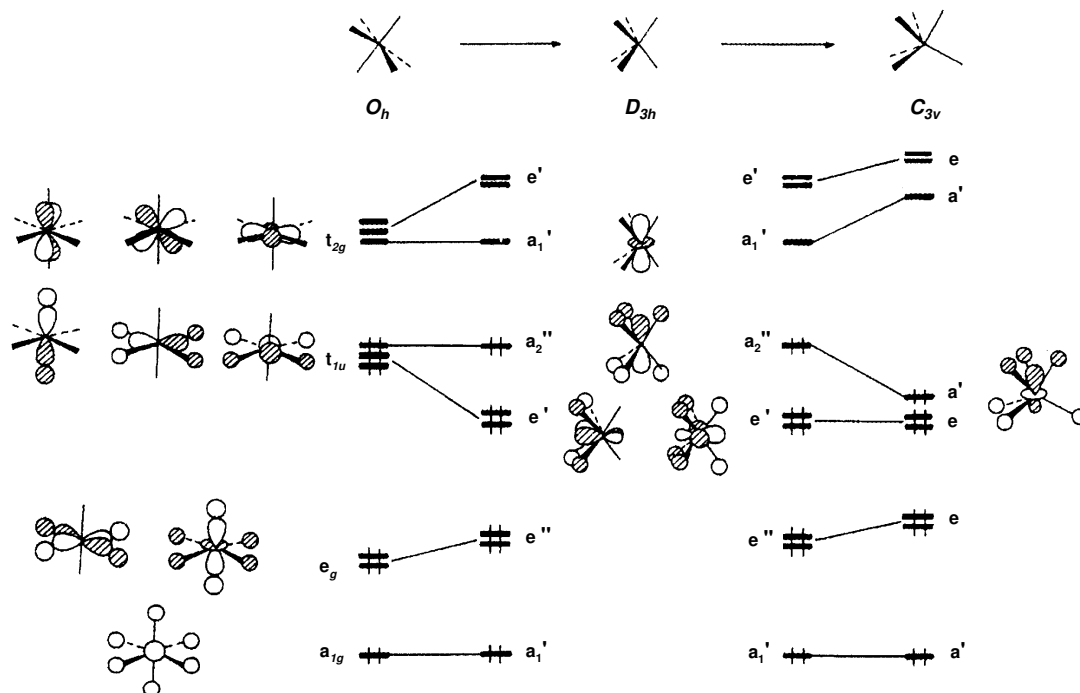


**Figure 3.** Orbital correlation diagram for the distortion of a  $d^0$   $MH_6$  molecule from  $O_h$  to  $D_{3h}$  to  $C_{3v}$  geometries (taken from ref. [9]).

M. Kaupp<sup>[11]</sup> added the following observations: The energy gain from a trigonal distortion of the regular prism (i.e.  $a_1'$  to  $a'$  in figure 3) is much less with bulkier ligands (like  $CH_3$  compared against H) due to agostic interactions ( $C-H \rightarrow W$ ) and tends to facilitate the distortion, whereas  $\pi$ -donation contributions from nonbonding ligand orbitals (e.g. in  $WF_6$ ) favor more symmetrical structures (like  $O_h$ ).

In a recent publication K. Seppelt<sup>[24]</sup> summarizes all these facts.  $WH_6$  and  $W(CH_3)_6$  are  $C_{3v}$  with a distorted trigonal prismatic structure. Hexamethyl anionic complexes are undistorted trigonal prisms. Addition of one electron to the system, going from  $W(CH_3)_6$

to  $\text{Re}(\text{CH}_3)_6$ , also removes the distortion. And finally, the distortion of second-row transition metal compounds seems to be a little stronger than that for identical third-row compounds. Compounds with ligands that can  $\pi$ -bond ( $-\text{OR}$ , and  $-\text{NR}_2$  for example) have  $O_h$  structures. If all orbitals in an 18 electron valence system like  $\text{W}(\text{CO})_6$  are occupied, then the octahedral geometry prevails (see figure 3). That  $\text{WF}_6$  is octahedral can be explained by the fact that there is considerable back-donation of electron density from the F ligands to the central atom via  $\pi$ -bonding and also because there is a considerable ligand-ligand repulsion as a consequence of the partial negative charge on the fluorine atoms. This is not the case in  $\text{W}(\text{CH}_3)_6$  because it can not form  $\pi$ -bonds, therefore it is a 12 electron system in which the  $C_{3v}$  geometry will prevail.

## 2.2 $\text{MoF}_6$ and $\text{WF}_6$ derivatives with $-\text{OCH}_2\text{CF}_3$ , $-\text{OC}_6\text{F}_5$ and $-\text{OC}(\text{CF}_3)_3$ groups as ligands

Tungsten hexaphenoxide was first reported in the literature in 1937.<sup>[25]</sup> Many other alkoxy- and phenoxy- tungsten (VI) and molybdenum (VI) derivatives were synthesized later in the 70's.<sup>[26-28]</sup> Based on  $^{19}\text{F}$  NMR spectroscopy, these compounds were characterized as monomeric octahedral species. Many other similar complexes of this type have been synthesized and characterized ever since, still nothing has changed, they are all octahedral.<sup>[29-39]</sup>

As it is stated in the literature,  $\text{MoF}_6$  and especially  $\text{WF}_6$  are good starting materials for a stepwise nucleophilic substitution using alkoxy- and phenoxy- groups due to the fact that they have relatively small oxidation strengths compared to other hexafluorides.<sup>[38]</sup>

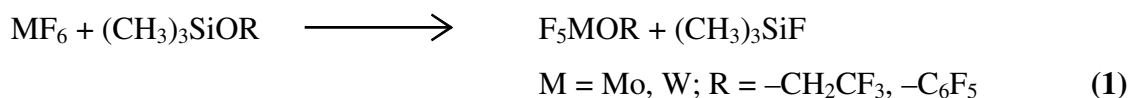
While there is no doubt that  $\text{MoF}_6$  and  $\text{WF}_6$  and its alkoxy- and phenoxy- derivatives which carry non bonding electron pairs on the ligands are octahedral, the question that raises here is how close in energy a trigonal prismatic structure would be. If it is close to  $10 \text{ kcal mol}^{-1}$ , then it can be assumed that the molecules would show fluxionality already at ambient or slightly elevated temperatures, so that they can be called non rigid. This is difficult to prove by experiments, since in  $\text{MoF}_6$  and  $\text{WF}_6$  all fluorine atoms remain equal before and after the rearrangement. Therefore this problem was solved by a typical

chemical approach, namely the substitution of one fluorine atom by a ligand with similar chemical behavior. The auxiliary ligands  $-\text{OCH}_2\text{CF}_3$ ,  $-\text{OC}_6\text{F}_5$ , and  $-\text{OC}(\text{CF}_3)_3$  were chosen since they are fairly easy to introduce, and the resulting compounds are at least in part stable enough for subsequent high temperature NMR investigations.

Molecules of the type  $\text{F}_5\text{M}(\text{R})$  with  $\text{M} = \text{Mo}$  or  $\text{W}$ ,  $\text{R} = -\text{OCH}_2\text{CF}_3$  or  $-\text{OC}_6\text{F}_5$ , and  $\text{F}_5\text{WOC}(\text{CF}_3)_3$  were successfully synthesized and characterized (see experimental section). All molecules have an octahedral ground state structure as seen by the  $^{19}\text{F}$  NMR spectra and crystallographic data; at elevated temperatures the non equivalent metal bonded fluorine atoms undergo an intramolecular exchange. NMR simulations of the  $^{19}\text{F}$  spectra using either the Bailar twist (3:3) or the 2:4 exchange mechanisms provided the energy for such a rearrangement. Experimental values were compared against theoretical calculations, both being of the same magnitude and in quite good agreement with each other. As far as it is known, this experimental determination of such an energy barrier is the first case of an experimental proof for the octahedral-trigonal prismatic rearrangement.

### 2.2.1 Preparation of $\text{F}_5\text{Mo}(\text{OCH}_2\text{CF}_3)$ , $\text{F}_5\text{W}(\text{OCH}_2\text{CF}_3)$ , $\text{F}_5\text{Mo}(\text{OC}_6\text{F}_5)$ , $\text{F}_5\text{W}(\text{OC}_6\text{F}_5)$ , and $\text{F}_5\text{W}(\text{OC}(\text{CF}_3)_3)$ , structural determinations

These monosubstituted derivatives of  $\text{MoF}_6$  and  $\text{WF}_6$  were prepared using modifications on literature procedures (see experimental section) and according to reaction schemes (1) and (2).



$\text{LiOC}(\text{CF}_3)_3$  gave just the tungsten derivative, however it does not react with  $\text{MoF}_6$ . Under suitable conditions (see experimental section) only single substitution is observed. Four of these compounds are liquids at room temperature,  $\text{F}_5\text{Mo}(\text{OC}_6\text{F}_5)$  is a solid. All are characterized by  $^{19}\text{F}$  NMR and vibrational spectra, elemental analyses, and a single

crystal structure determination in the case of  $F_5Mo(OC_6F_5)$ . The structure of all five compounds at the metal center is octahedral, as is evidenced by the  $AB_4$  type  $^{19}F$  NMR spectra at room temperature or below. Further proof comes from the single crystal structure determination of  $F_5Mo(OC_6F_5)$ , which delivers structural details, see table 1 and figure 4.

**Table 1.** Experimental bond lengths [pm] and selected angles [ $^\circ$ ] of  $F_5Mo(OC_6F_5)$  and *cis*-( $CF_3CH_2O$ ) $_2$ MoF $_4$

	$F_5Mo(OC_6F_5)$		<i>cis</i> -( $CF_3CH_2O$ ) $_2$ MoF $_4$
Mo–O	182.7(2)		178.5(4)-179.2(4)
Mo–F <sub>ax</sub>	184.4(2)		184.7(4)-184.9(4)
Mo–F <sub>eq</sub>	182.7(2)-184.7(2)		184.0(4)-184.7(4)
C–O	133.0(3)		140.5(6)-142.1(7)
C–C	137.1(4)-139.8(4)		147.8(9)-150.9(9)
C–F	132.1(3)-133.0(3)		126.2(9)-133.5(8)
F <sub>ax</sub> –Mo–O	170.8(1)	O–Mo–O	98.2(2), 98.3(2)
F <sub>eq</sub> –Mo–O	85.8(1)-97.1(1)	F–Mo–F	83.8(2)-89.1(2), 171.8(2), 171.7(2)
Mo–O–C	149.8(2)		144.1(4), 144.7(4)

It may be of interest that  $F_5Mo(OC_6F_5)$  is deeply colored in the condensed phase. In the crystal structure an intermolecular interaction between the  $-C_6F_5$  ring of one molecule and the  $-OMoF_5$  group of another molecule is obvious, resulting in a charge transfer interaction, where the aromatic ring is obviously the donor and the  $-OMoF_5$  group the acceptor (Figure 4). Besides this finding the structure is completely as expected.

Reaction between  $MoF_6$  and  $(CF_3CH_2O)Si(CH_3)_3$  does not produce solely  $F_5Mo(OCH_2CF_3)$ . Upon longer reaction times at room temperature and especially if  $(CF_3CH_2O)Si(CH_3)_3$  is applied in excess, *cis*-( $CF_3CH_2O$ ) $_2$ MoF $_4$  is detectable as a byproduct. This is indicated by the  $A_2B_2$  spectrum of the molybdenum bonded fluorine



atoms (see experimental section). This compound crystallizes spontaneously from the reaction mixture, and numerical values of the single crystal structure determination are collected in table 1 above. The *cis*-orientation within the octahedral molybdenum environment of the two  $-\text{OCH}_2\text{CF}_3$  groups is confirmed, see figure 5.

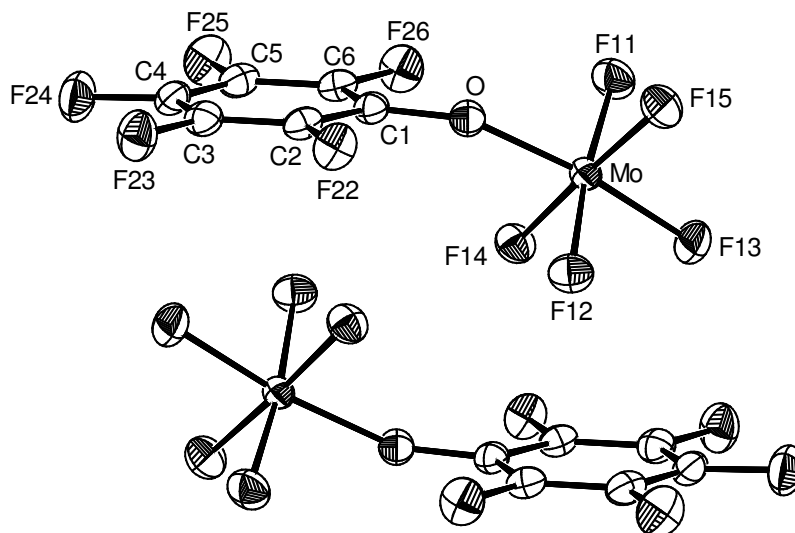


**Figure 4.** Crystal structure of  $\text{F}_5\text{Mo}(\text{OC}_6\text{F}_5)$ , 50% probability plot. Shown is a pair of molecules that has a mutual charge transfer interaction resulting in a deep color. The second molecule is generated by the inversion center.

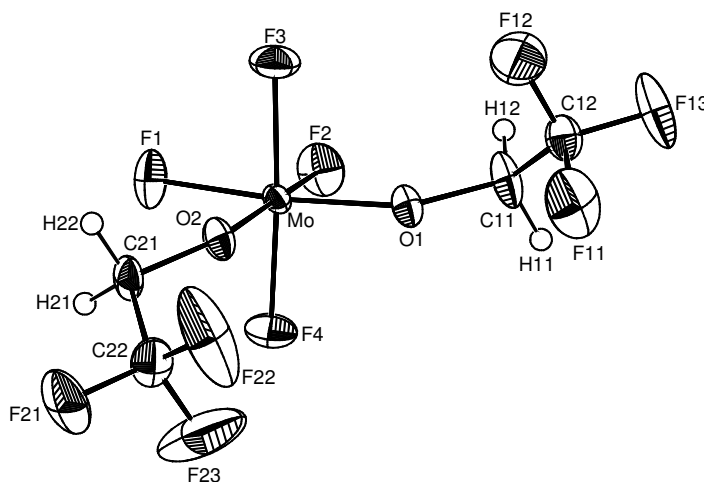


**Figure 5.** Crystal structure of *cis*- $(\text{CF}_3\text{CH}_2\text{O})_2\text{MoF}_4$ , 50% probability plot. Shown is molecule I. The crystallographically independent molecule II is very similar.

### 2.2.2 Theoretical predictions for MoF<sub>6</sub>, WF<sub>6</sub>, F<sub>5</sub>Mo(OCH<sub>2</sub>CF<sub>3</sub>), F<sub>5</sub>W(OCH<sub>2</sub>CF<sub>3</sub>), F<sub>5</sub>Mo(OC<sub>6</sub>F<sub>5</sub>), F<sub>5</sub>W(OC<sub>6</sub>F<sub>5</sub>), F<sub>5</sub>Mo(OC(CF<sub>3</sub>)<sub>3</sub>), and F<sub>5</sub>W(OC(CF<sub>3</sub>)<sub>3</sub>)

Based on previous studies,<sup>[12,13,40]</sup> all calculations were done on the density functional level of theory, method Becke 3LYP.<sup>[41,42]</sup> This method combined with the 6–311G(d,p) basis set implemented in the GAUSSIAN<sup>[43]</sup> program provided a fairly good approximation to experimental values, but the bond lengths are overestimated somehow as it is stated in the literature<sup>[40]</sup> (compare also the crystal structure of F<sub>5</sub>Mo(OC<sub>6</sub>F<sub>5</sub>) obtained and its theoretical calculation in the upcoming section). For the metal atoms ECP's were used (see experimental section for details). In most of the cases a successful optimization with the highest possible symmetry failed, therefore the symmetry had to be lowered or even set at C<sub>1</sub>.

As expected the ground state for MoF<sub>6</sub> and WF<sub>6</sub> (as well for CrF<sub>6</sub>, NbF<sub>6</sub><sup>-</sup>, TcF<sub>6</sub><sup>+</sup>, and ReF<sub>6</sub><sup>+</sup>)<sup>[44]</sup> is octahedral. The calculated M–F bond distances come out about 4 pm longer than in the experiment, so far as experimental values are known (see table 2 and its references). The trigonal prismatic structure is in all cases a transition state, as is evidenced by one imaginary frequency. The M–F bond distances in the transition state are marginally longer than in the octahedral ground state, reflecting the small loss of energy. It is evident that in MoF<sub>6</sub> this *O<sub>h</sub>–D<sub>3h</sub>* barrier is even lower than in CrF<sub>6</sub> and WF<sub>6</sub>. The lower barrier in MoF<sub>6</sub> as compared to CrF<sub>6</sub> can be explained by the increased size of the MoF<sub>6</sub> molecule, which results in lesser interligand repulsion, making the trigonal prismatic structure more favorable. The higher barrier in WF<sub>6</sub> is explained by the influence of the strongly increased relativistic effect: The W–F bond lengths are hardly longer than the Mo–F bond lengths, but the polarity of the bond is increased, see table 2.<sup>[44]</sup>

In the isoelectronic series NbF<sub>6</sub><sup>-</sup>, MoF<sub>6</sub>, and TcF<sub>6</sub><sup>+</sup> the decreasing bond polarity favors the trigonal prismatic structure, so that for unknown TcF<sub>6</sub><sup>+</sup> the octahedral structure is no more guaranteed if the errors of the DFT calculations are taken somewhat generous.

**Table 2.** DFT-calculations on selected molecular, anionic and cationic hexafluorides: energies, bond distances, and lowest vibrational frequency (taken from ref. [44])

		Energy + zero point energy (a.u.)	$r_{M-F}$ (pm)	$\nu$ ( $\text{cm}^{-1}$ ) <sup>[a]</sup>	$\Delta E$ ( $\text{kcal mol}^{-1}$ )
CrF <sub>6</sub>	O <sub>h</sub>	-686.172442	174.0	129.9	0.0
	D <sub>3h</sub>	-686.152051	174.8	-97.5	12.7
MoF <sub>6</sub>	O <sub>h</sub>	-667.592595	186.6(182.0(3) <sup>[b]</sup> )	91.2 (116) <sup>[c]</sup>	0.0
	D <sub>3h</sub>	-667.582059	186.9	-49.0	6.6
WF <sub>6</sub>	O <sub>h</sub>	-666.564772	187.5 (183.2(3) <sup>[d]</sup> )	111.5 (127) <sup>[c]</sup>	0.0
	D <sub>3h</sub>	-666.547373	188.0	-75.5	10.9
NbF <sub>6</sub> <sup>-</sup>	O <sub>h</sub>	-656.667833	193.9	99.3	0.0
	D <sub>3h</sub>	-656.651896	194.2	-74.5	10.0
TcF <sub>6</sub> <sup>+</sup>	O <sub>h</sub>	-679.601872	182.6	76.5	0.0
	D <sub>3h</sub>	-679.594678	183.1	-39.0	4.4
ReF <sub>6</sub> <sup>+</sup>	O <sub>h</sub>	-677.203127	183.4	109.1	0.0
	D <sub>3h</sub>	-677.188196	184.1	-72.0	9.4

[a] lowest calculated vibrational frequencies, T<sub>2u</sub> in O<sub>h</sub>, imaginary frequencies A<sub>1</sub><sup>u</sup> in D<sub>3h</sub>

[b] experimental value, see ref.[45]

[c] experimental value, see ref. [45,46]

[d] experimental value, see ref. [45,47]

Looking at all known hexafluorides (except XeF<sub>6</sub>), clearly reveals the exceptional case of MoF<sub>6</sub>. The  $\nu_6$  (T<sub>2u</sub>) vibration (both i.r. and Raman forbidden) of these octahedral molecules has the lowest value for MoF<sub>6</sub>, see table 3. This is so since this vibration contributes to the octahedral-trigonal prismatic rearrangement, see figure 6. (For simplification the structures of the  $d^1$ - $d^4$  hexafluorides ReF<sub>6</sub>-PtF<sub>6</sub>, TcF<sub>6</sub>-RhF<sub>6</sub> are considered octahedral, although some of them may exhibit very small *Jahn-Teller* distortions.<sup>[40,48-50]</sup>)

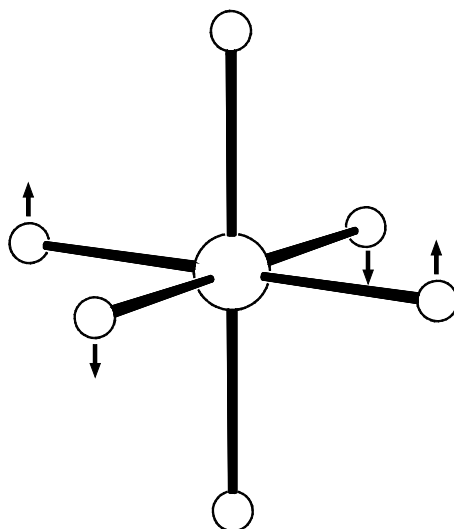


**Figure 6.** The Raman and i.r. forbidden  $\nu_6(T_{2u})$  vibration of the octahedron, which is one component of both the Bailar and 2:4 rearrangement.

**Table 3.** Experimental Values [ $\text{cm}^{-1}$ ] for the Raman and i.r forbidden  $\nu_6(T_{2u})$  vibration of molecular octahedral hexafluorides.<sup>[46]</sup>

					SF <sub>6</sub> 347
					SeF <sub>6</sub> 264
	MoF <sub>6</sub> 116	TcF <sub>6</sub> 145	RuF <sub>6</sub> <sup>(a)</sup> 186	RhF <sub>6</sub> <sup>(a)</sup> 192	TeF <sub>6</sub> 197
	WF <sub>6</sub> 127	ReF <sub>6</sub> 193	OsF <sub>6</sub> <sup>(a)</sup> 205	IrF <sub>6</sub> <sup>(a)</sup> 206	PtF <sub>6</sub> <sup>(a)</sup> 211
	UF <sub>6</sub> 142	NpF <sub>6</sub> 164	PuF <sub>6</sub> 173		

<sup>(a)</sup> See references given in ref. [46].

The DFT calculations of the monosubstituted derivatives  $F_5Mo-OR$  and  $F_5W-OR$  are summarized in table 4. Again the major difference is that experimental  $Mo-F$  bond lengths are a few pm shorter than calculated. The energy difference between octahedral ground state and trigonal prismatic excited state is calculated around  $10 \text{ kcal mol}^{-1}$  for the three molybdenum compounds and around  $15 \text{ kcal mol}^{-1}$  for the three tungsten compounds.

**Table 4.** Results of DFT calculations on  $F_5M(OCH_2CF_3)$ ,  $F_5M(OC_6F_5)$ , and  $F_5M(OC(CF_3)_3)$ ,  $M = Mo, W$ .

Complex <sup>a</sup>	Energy + zero point energy (a.u)	$\Delta E$ (kcal mol <sup>-1</sup> )	bond distances (pm)	
$CF_3-CH_2-O-MoF_5$ Oct.	-1019.983954	0	Mo-O	185.2
			Mo-F <sub>ax</sub>	187.2
			Mo-F <sub>eq</sub>	187.2-190.2
			C-O	140.3
$CF_3-CH_2-O-MoF_5$ Tp.	-1019.967650	10.23	Mo-O	188.2
			Mo-F <sub>1,2,3</sub>	187.0-187.8
			Mo-F <sub>4,5</sub>	189.2
			C-O	141.6
$CF_3-CH_2-O-WF_5$ Oct.	-1018.951387	0	W-O	186.0
			W-F <sub>ax</sub>	188.4
			W-F <sub>eq</sub>	188.1-190.3
			C-O	140.5
$CF_3-CH_2-O-WF_5$ Tp.	-1018.928884	14.12	W-O	188.8
			W-F <sub>1,2,3</sub>	188.1-188.8
			W-F <sub>4,5</sub>	190.1
			C-O	141.9
$C_6F_5-O-MoF_5$ Oct.	-1370.901500	0	Mo-O	188.4
			Mo-F <sub>ax</sub>	186.8
			Mo-F <sub>eq</sub>	187.4-189.9
			C-O	132.3
$C_6F_5-O-MoF_5$ Tp.	-1370.88428	10.81	Mo-O	193.6
			Mo-F <sub>1,2,3</sub>	186.6-187.6
			Mo-F <sub>4,5</sub>	189.0-189.1
			C-O	133.4

Continuation table 4.

C <sub>6</sub> F <sub>5</sub> -O-WF <sub>5</sub> Oct.	-1369.867201	0	W-O	187.4
			W-F <sub>ax</sub>	187.9
			W-F <sub>eq</sub>	188.4-189.2
			C-O	133.2
C <sub>6</sub> F <sub>5</sub> -O-WF <sub>5</sub> Tp.	-1369.842479	15.51	W-O	191.8
			W-F <sub>1,2,3</sub>	188.0-188.6
			W-F <sub>4,5</sub>	189.5
			C-O	135.0
(CF <sub>3</sub> ) <sub>3</sub> C-O-MoF <sub>5</sub> Oct.	-1694.214825	0	Mo-O	186.5
			Mo-F <sub>ax</sub>	186.6
			Mo-F <sub>eq</sub>	187.4-187.7
			C-O	137.9
(CF <sub>3</sub> ) <sub>3</sub> C-O-MoF <sub>5</sub> Tp.	-1694.194078	13.02	Mo-O	186.5
			Mo-F <sub>1,2,3</sub>	187.4-187.7
			Mo-F <sub>4,5</sub>	187.5, 186.6
			C-O	137.9
(CF <sub>3</sub> ) <sub>3</sub> C-O-WF <sub>5</sub> Oct.	-1693.184774	0	W-O	187.2
			W-F <sub>ax</sub>	187.6
			W-F <sub>eq</sub>	188.3-188.4
			C-O	138.1
(CF <sub>3</sub> ) <sub>3</sub> C-O-WF <sub>5</sub> Tp.	-1693.158812	16.29	W-O	188.7
			W-F <sub>1,2,3</sub>	188.3-189.7
			W-F <sub>4,5</sub>	188.7, 188.8
			C-O	138.4

<sup>a</sup> Oct = octahedral, Tp = trigonal prismatic.

### 2.2.3 Dynamic <sup>19</sup>F NMR spectra of F<sub>5</sub>Mo(OCH<sub>2</sub>CF<sub>3</sub>), F<sub>5</sub>W(OCH<sub>2</sub>CF<sub>3</sub>), F<sub>5</sub>Mo(OC<sub>6</sub>F<sub>5</sub>), F<sub>5</sub>W(OC<sub>6</sub>F<sub>5</sub>), and F<sub>5</sub>W(OC(CF<sub>3</sub>)<sub>3</sub>)

Before going into details about all simulations performed, some aspects of Dynamic NMR (DNMR) are presented below. The reader who is already familiar with this topic and words like *topomers*, *activation parameters*, *coalescence*, *Arrhenius plot*, *Eyring equation*, and *Eyring plot*, might omit this introduction, turn some pages ahead and continue reading the <sup>19</sup>F DNMR for the compounds of interest.

The history of DNMR is as old as the history of NMR itself.<sup>[51,52]</sup>  $^1\text{H}$  DNMR started gaining attention in the late 1950's and at the end of the 1960's it was already well established that this kind of spectroscopy could be used to determine energy barriers ranging from 5-6 kcal mol<sup>-1</sup> up to 20-25 kcal mol<sup>-1</sup>.<sup>[51]</sup> In the early 1970's  $^{13}\text{C}$  DNMR spectroscopy began to develop and the first activation parameters for the chair-to-chair interconversion in some cyclohexanes derivatives were obtained.<sup>[52]</sup>

Rate processes involving reversible intermolecular proton transfer, rotations around sterically crowded single bonds and single bonds with partial double character, inversion of lone electron pairs on rings, and intramolecular rearrangements were at that time among the most common examples studied by this kind of spectroscopy. At the present time it is well known that dynamic nuclear magnetic resonance is also capable of yielding quantitative data about rate constants and activation parameters.<sup>[51-54]</sup>

DNMR even led to the discovery of a new class of compounds, molecules with fluxional structures, of which bullvalene<sup>[55]</sup> was at that time perhaps the most striking example.<sup>[51]</sup> Ever since, it has been used to study intermolecular exchange like proton exchange between acids, ligand exchange in inorganic and metalorganic complexes, dissociation of covalent bonds into ions and recombination of the later ones, and of course intramolecular exchange.<sup>[56]</sup> For the case of intramolecular exchange in which the atoms of a molecule just permute their positions, the word *Topomer(s)* has been used in the literature to describe such species.<sup>[56,57]</sup>

Ever since DNMR started gaining interest there have been many hundreds of publications dealing with this topic. Intramolecular rearrangements in molecules of the type  $\text{PF}_3(\text{NR}_2)_2$ ,<sup>[58]</sup>  $\text{SF}_3(\text{R})$ ,<sup>[59]</sup>  $\text{SF}_4$ ,<sup>[60]</sup> and even complexes of the type  $\text{ML}_5$ <sup>[61]</sup> and  $\text{H}_2\text{M}[\text{PR}_3]_4$ ,<sup>[62]</sup> for instance, have been thoroughly studied. *Activation parameters* ( $\Delta G^\ddagger$ ,  $\Delta H^\ddagger$ ,  $\Delta S^\ddagger$ ,  $E_A$ ) have been calculated and the elucidation of a mechanism for the intramolecular interconversion has been determined in many cases successfully with dynamic NMR spectroscopic techniques.<sup>[58-65]</sup>

To determine the activation energy and other activation parameters many approaches and methods have been used depending on the system being studied.<sup>[52]</sup> Obtaining a rate

constant ( $k$ ) at one specific temperature may be of interest, but in most cases more interesting information is obtained from an analysis of the energy quantities involved in the whole process.<sup>[52,54]</sup> In most of the cases this is achieved by varying the temperature of the sample and recording its NMR spectra at the desired temperature.<sup>[51,53,54]</sup> The range of rates observable by NMR depends on the separation, in hertz, of the resonance of the nuclei involved in the dynamic process. The separation, in turn, depends on the strength of the magnetic field used to observe the nuclei, the nature of the nucleus, and the chemical environment of each nucleus involved.<sup>[54]</sup>

Raising the temperature of the sample produces a loss of the fine structure of the NMR signals. If two nuclei, A and B both of the same isotope, for instance  $^{19}\text{F}$ , but in different chemical environments, are exposed to a magnetic field, each of them will experience a different induced magnetic field and each will have a different set of energy levels. If the nuclei remain in their static environment (for example at low temperatures), each will undergo a transition and each will produce a single resonance. However, if the nuclei are free to exchange places (for example at higher temperatures) and if the exchange rate occurs more rapidly than the time each nucleus spends in the ground state, the resonance broaden, move toward one another, and, at a high enough rate, a single line will exist.<sup>[54]</sup> The temperature at which two peaks (NMR signals) merge into one, i.e., the “valley” between the two separate peaks disappears is defined as the *coalescence* temperature.<sup>[66]</sup>

In early studies the activation energy ( $E_A$ ) was determined from the *Arrhenius equation* (i), where A (frequency factor) and  $E_A$  are customarily obtained from a linear plot of  $\ln(k)$  versus  $\frac{1}{T}$ , known as the *Arrhenius plot*.<sup>[53,56,63]</sup>

$$k = Ae^{-E_A/RT} \quad (\text{i})$$

However, it was rather early realized that eq. (i) rests on over-simplified assumptions, and that a more realistic treatment could be based on statistical thermodynamics. The absolute rate theory, developed by Eyring is well suited for the treatment of the type of problems of interest in the present context.



The fundamental equation in this theory is the so called *Eyring equation*, eq. **(ii)**,<sup>[51,53,54,56,63]</sup> where  $\kappa$  is the so called transmission coefficient, which for simplicity has been used in the literature as 1,  $k_B$  is the Boltzmann constant,  $T$  the absolute temperature,  $R$  the ideal gas constant and  $h$  the Planck constant.<sup>[51,53,54,63]</sup>

$$k = \kappa \frac{k_B T}{h} \exp^{(-\Delta G^\ddagger / RT)} \quad \text{(ii)}$$

Equation **(ii)** can be written in terms of enthalpies and entropies, since

$$\Delta G^\ddagger = \Delta H^\ddagger - T\Delta S^\ddagger \quad \text{(iii)}$$

thus taking the form of

$$k = \kappa \frac{k_B T}{h} \exp^{(-\Delta H^\ddagger + T\Delta S^\ddagger) / RT} \quad \text{(iv)}$$

which can be linearized to the following form

$$\ln\left(\frac{k}{T}\right) = -\frac{\Delta H^\ddagger}{RT} + \ln\left(\frac{\kappa k_B}{h}\right) + \frac{\Delta S^\ddagger}{R} \quad \text{(v)}$$

Temperature independent  $\Delta H^\ddagger$  and  $\Delta S^\ddagger$  values can be obtained experimentally in a direct fashion. There are two ways to do this. One can make use of the linearized Eyring eq.

**(v)** and plot  $\ln\left(\frac{k}{T}\right)$  versus  $\frac{1}{T}$  to give a straight line with the slope  $-\frac{\Delta H^\ddagger}{R}$  and intercept

$\ln\left(\frac{\kappa k_B}{h}\right) + \frac{\Delta S^\ddagger}{R}$ , or one may calculate  $\Delta G^\ddagger$  from eq. **(ii)** for each temperature and plot eq. **(iii)**.<sup>[51,53,54]</sup>

The usual procedure for a total line shape analysis is to generate and plot a series of line shapes, each of which corresponds to a different exchange rate. Each plot is then compared with the actual shape of the resonances (i.e. experimental spectra) at a particular temperature. The closest fit may be determined visually, by least-square comparisons or by some other technique designed to minimize the differences between

certain features of the plotted and actual spectra.<sup>[54,56]</sup>

In the case of the complexes studied here a visual comparison between experimental and simulated spectra was carried out. All kinds of line shape analysis or least-square comparisons were unsuccessful due to the fact that experimental spectra show a broadening at the base of the signals, especially at room temperature or below. This broadening makes it impossible for the simulation program gNMR<sup>[67]</sup> to perform any kind of least-square analysis.

The broadening of the signals is attributed to the following facts: The samples needed to be measured inside PFA (Perfluoro-alkoxy polymer, see experimental section) inserts due to their high reactivity towards glass and even quartz. These PFA tubes might appear straight to the naked eye, but are not necessarily straight for the NMR machine. Thus a gradient in the magnetic field is experienced by the sample and therefore the so called non-lorentzian type signals arise.<sup>[51,67b]</sup> Another possible explanation for such asymmetry in the experimental signals is the fact that an automatic shim of the lock signal in the NMR machine was used instead of performing a manual shim.<sup>[67b]</sup> Never the less, the higher the temperature the better simulated and experimental spectra were matched. Figure 7 shows an example of this non-lorentzian shape<sup>[51]</sup> of the experimental signals for  $F_5Mo(OC_6F_5)$  at 20 °C and at a higher temperature. For simplicity and comparison means, the B<sub>4</sub>- and A- part of the <sup>19</sup>F NMR spectra are set to the same intensity for the 20 °C example.

It is clearly evident that all five compounds studied here exhibit strongly temperature dependent <sup>19</sup>F NMR spectra of the metal bonded fluorine atoms, while the typical <sup>19</sup>F NMR (and <sup>1</sup>H NMR) spectra of the  $-OCH_2CF_3$ ,  $-OC_6F_5$ , and  $-OC(CF_3)_3$  groups are less sensitive towards temperature and hence insignificant for this study. The numerical data of these groups are given in the experimental section and will not be discussed any further.

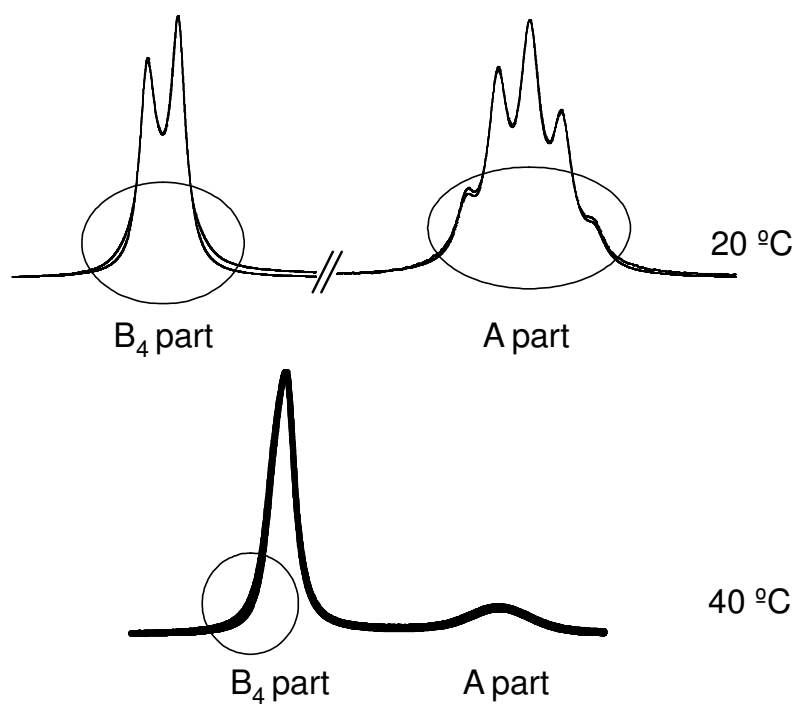


**Figure 7.** Over imposed experimental and simulated  $^{19}\text{F}$  NMR spectra for  $\text{F}_5\text{Mo}(\text{OC}_6\text{F}_5)$  at two different temperatures showing the non-lorentzian shapes of the experimental spectra, arbitrary scales.

The typical  $\text{AB}_4$  spectra (approximately: doublet + quintet) of the  $-\text{OMF}_5$  group are best resolved at room temperature or below. Upon warming line broadening takes place. The A- and the  $\text{B}_4$ -parts exhibit intrinsic shifts up field with increasing temperature, with the apical fluorine being more sensitive than the four equatorial fluorine atoms. Consequently the second order character of the underlying  $\text{AB}_4$ -spectrum increases since  $\Delta_\delta = \delta_{\text{B}_4} - \delta_{\text{A}}$  decreases with increasing temperature. At higher temperatures coalescence is observed and further heating results in a sharpening of the remaining single line.

All simulated and experimental spectra, as well as the rate constant obtained for each temperature can be seen in figures 8-12. A detailed description of the simulations is given in the experimental section. The most important parameters like sample concentration, chemical shifts, coupling constants and line widths which are needed to

produce each of the simulated spectra can be seen in detail also in the experimental section.

Due to the fact that there is an intrinsic chemical shift of the apical and equatorial fluorine atoms with increasing temperature, the chemical shifts of both the A- and B<sub>4</sub>-parts have to be adjusted in the simulated spectra for each experimental spectra studied. Nevertheless, this intrinsic chemical shift of the mentioned parts does not affect significantly the determination of the activation parameter ( $\Delta H^\ddagger$ ) that was calculated, but indeed it makes the simulations more complicated.

Only in the case of F<sub>5</sub>W(OC<sub>6</sub>F<sub>5</sub>) the high temperature limit of the spectra could be obtained, since the spectrometers used have an upper temperature limit of 185 °C for the 90 MHz and of 150 °C for the 400 MHz instrument. The molybdenum compounds, in particular, start to decompose at these elevated temperatures.

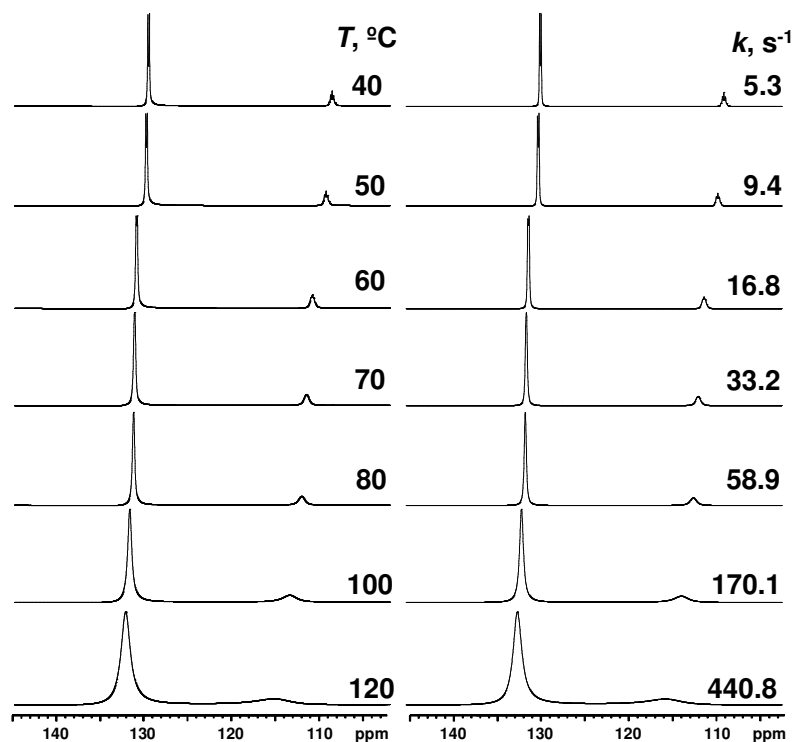


**Figure 8.** Experimental (left) and simulated (right) temperature dependent 376 MHz <sup>19</sup>F NMR spectra of F<sub>5</sub>W(OCH<sub>2</sub>CF<sub>3</sub>).

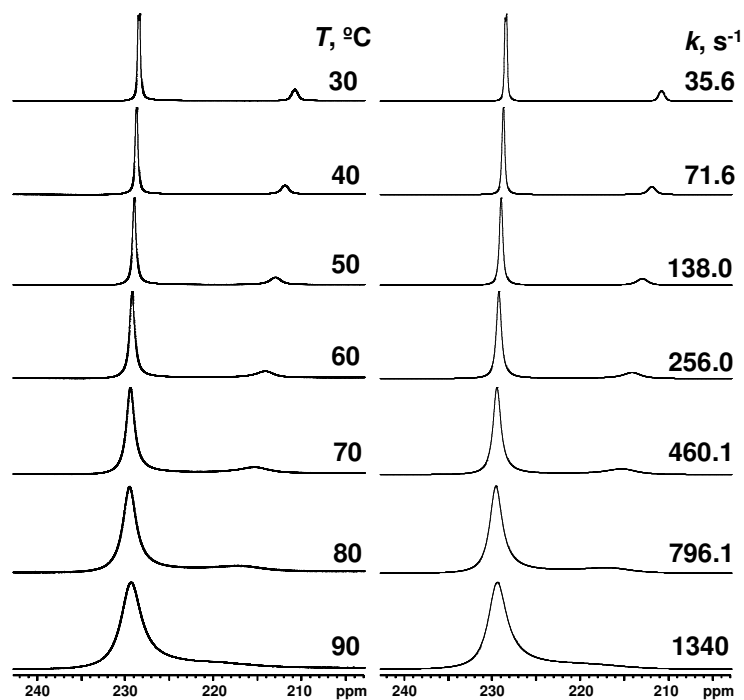


**Figure 9.** Experimental (left) and simulated (right) temperature dependent 376 MHz  $^{19}\text{F}$  NMR spectra of  $\text{F}_5\text{Mo}(\text{OCH}_2\text{CF}_3)$ .

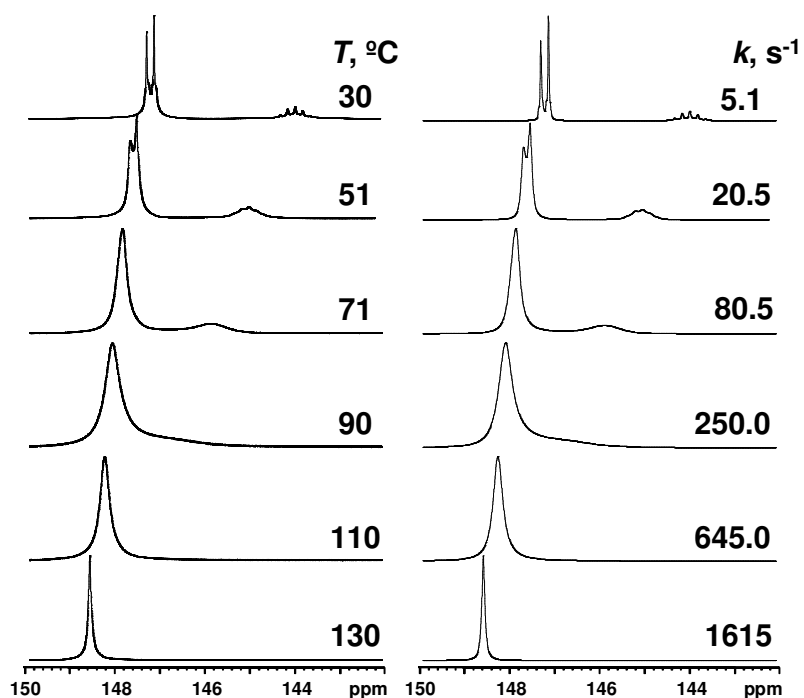


**Figure 10.** Experimental (left) and simulated (right) temperature dependent 376 MHz  $^{19}\text{F}$  NMR spectra of  $\text{F}_5\text{W}(\text{OC}_6\text{F}_5)$ .

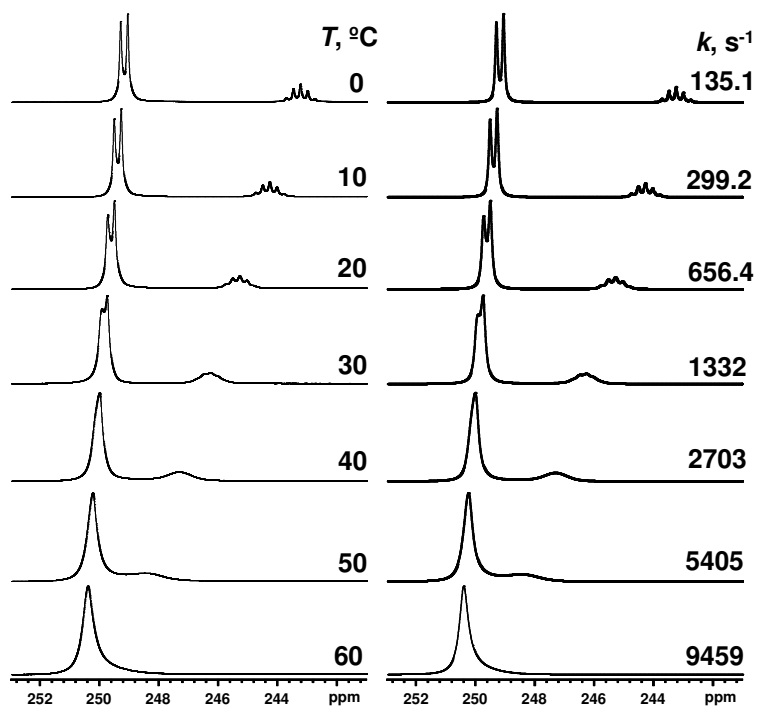


**Figure 11.** Experimental (left) and simulated (right) temperature dependent 376 MHz  $^{19}\text{F}$  NMR spectra of  $\text{F}_5\text{Mo}(\text{OC}_6\text{F}_5)$ .

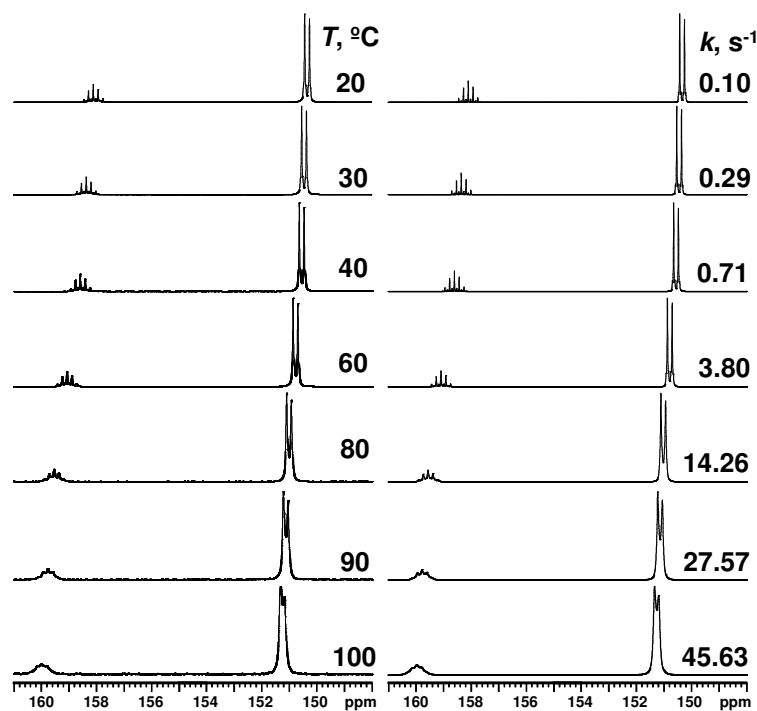


**Figure 12.** Experimental (left) and simulated (right) temperature dependent 376 MHz  $^{19}\text{F}$  NMR spectra of  $\text{F}_5\text{W}(\text{OC}(\text{CF}_3)_3)$ .

Obviously there occurs fluorine exchange of the metal bonded fluorine atoms. At first, the question that needs to be addressed is whether this exchange is intra- or intermolecular. There are three main reasons to support the intramolecular exchange: first, in the case of  $F_5W(OC_6F_5)$  we can give definite proof that the exchange is intramolecular. The tungsten bonded fluorine atoms have satellites of  $^{183}W$  ( $I = 1/2$ , 14% natural abundance).<sup>[68]</sup> These side bands are still visible in the high temperature limit (Figure 13), which shows that the five fluorine atoms remain bonded to the tungsten atom. For the molybdenum atoms this method is not available, since the satellites of the only NMR active isotopes of Mo ( $^{95/97}Mo$ ,  $I = 5/2$ , 15.9, 9.6 % nat. abundance)<sup>[68]</sup> are not observed except in highly symmetric molecules as in  $MoF_6$ .

Second, in the case of  $F_5Mo(OC_6F_5)$  temperature dependent  $^{19}F$  NMR spectra in different concentrations in different solvents ( $C_2D_2Cl_4$  and  $CD_2Cl_2$ ) did not show any concentration dependence, which is also an argument for intramolecular exchange.<sup>[67b,69]</sup> The energy value obtained for the exchange of both simulations is exactly the same within the experimental errors. Here are only presented the simulations of the  $C_2D_2Cl_4$  solution. The most important parameters for the  $CD_2Cl_2$  solution which are needed to produce each of the simulated spectra can be seen in details in the experimental section.

There is yet another argument in favor of intramolecular exchange: If one assumes that upon heating the metal bonded fluorine atoms could move from one metal atom to another, so would the  $-OR$  groups. This would result in a scrambling of F and OR groups and therefore in the formation of some or all members of the series  $F_{6-n}M(OR)_n$  ( $n = 2-6$ ). This is indeed observed, however, only at temperatures above  $100^\circ C$  and at a very slow rate, so that no coalescence of this type is seen.

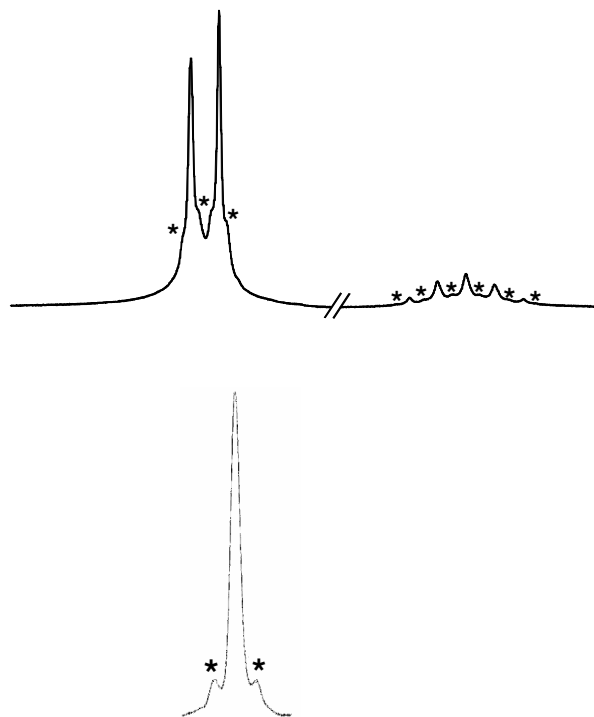


**Figure 13.** The low (30°C) and high temperature (184°C) limit  $^{19}\text{F}$  NMR (84.25MHz) spectra of  $\text{F}_5\text{W}(\text{OC}_6\text{F}_5)$  at high resolution, showing the  $^{183}\text{W}$ - $^{19}\text{F}$  satellite lines, marked by \*, arbitrary scales.

The  $^{19}\text{F}$  NMR spectra were simulated successfully (see figures 8-12 above) using the program gNMR.<sup>[67]</sup> Spin enumeration and permutational operators used for gNMR assuming the afore mentioned Bailar twist (3:3) or 2:4 torsional mechanisms as defined in figure 14 were employed.

The exact mechanism of the ligand exchange in the molecules studied is difficult to prove, in contrast to five coordinated species like  $\text{PF}_5$ ,<sup>[70]</sup> where a 2+2 exchange mechanism (*Berry* Pseudorotation)<sup>[70b]</sup> can be differentiated from a 3+2 exchange mechanism (*Turnstile* rotation).<sup>[70b]</sup> Simulated dynamic  $^{19}\text{F}$  NMR spectra for  $\text{F}_5\text{M-OR}$  molecules under the assumption of these two mechanisms (Bailar twist and 2:4) show no difference, so experimentally they are indistinguishable (for comparison see Appendix I).



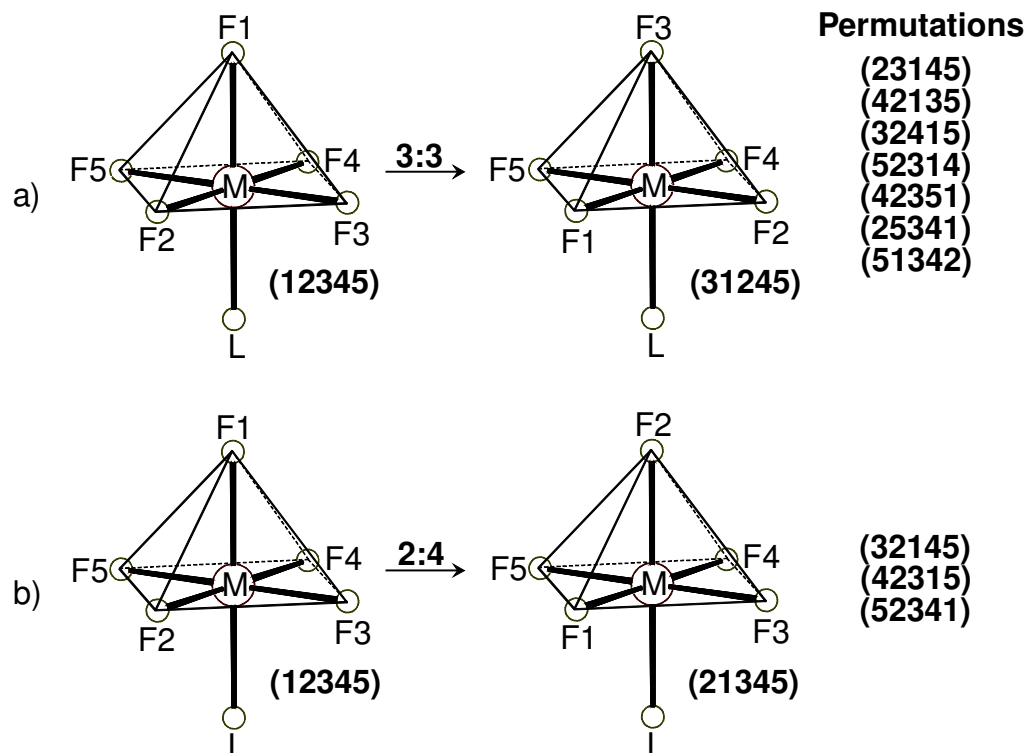


**Figure 14.** Definition of permutation operators used to describe the Bailar twist (3:3) and 2:4 exchange for compounds of the type  $F_5M-OR$  ( $R = -CH_2CF_3, -C_6F_5$ ,  $M = Mo, W$ ) and  $F_5W-OC(CF_3)_3$ .

In order to determine the activation parameters a set of rate constants has to be chosen. The preferred and chosen sets of  $k$  values presented here were derived from the Bailar twist torsion mechanism. The argument favoring the 3:3 mechanism is derived by theoretical calculations: All calculated trigonal prismatic structures discussed here have one imaginary frequency (i.e. transition state), and the vector of this vibration is identical to the reaction coordinate of the Bailar twist.

In fact it is seen from the simulations that the 2:4 torsion mechanism produces a series of rate constants ( $k$ ) that obey the following equation:

$$k_{2:4} = 2k_{3:3} \quad (\text{vi})$$

which indeed says that the 2:4 exchange mechanism goes twice as fast as the Bailar twist. If one thinks in terms of operators, it is clearly evident that the 3:3 mechanism has twice the amount of operators than the 2:4 mechanism. This might explain why the later is twice as fast as the former. A complete set of rate constants using the 2:4 mechanism for a selected compound can be seen in the Appendix I.

A series of meticulous simulations yielded rate constants for specific temperatures, as shown in table 5. Using the standard linearized Eyring equation (v) an Eyring plot for all compounds can be constructed, see figure 15.

Obviously an agreeable linear behavior is achieved by experiment. Linear regression “r” values (see Appendix II) are 0.9994 or higher for all the compounds studied. From the slope of these lines and with  $R = 0.00198582 \text{ kcal mol}^{-1} \text{ K}^{-1}$  the following data were found:  $\text{F}_5\text{Mo}(\text{OCH}_2\text{CF}_3)$  12.6,  $\text{F}_5\text{Mo}(\text{OC}_6\text{F}_5)$  (in  $\text{C}_2\text{D}_2\text{Cl}_4$ ) 12.3,  $\text{F}_5\text{Mo}(\text{OC}_6\text{F}_5)$  (in  $\text{CD}_2\text{Cl}_2$ ) 12.4,  $\text{F}_5\text{W}(\text{OCH}_2\text{CF}_3)$  13.0,  $\text{F}_5\text{W}(\text{OC}_6\text{F}_5)$  13.4, and  $\text{F}_5\text{W}(\text{OC}(\text{CF}_3)_3)$  15.9  $\text{kcal mol}^{-1}$ , which corresponds to  $\Delta H^\ddagger$  for the octahedral-trigonal prismatic rearrangement described before as the Bailar twist mechanism.

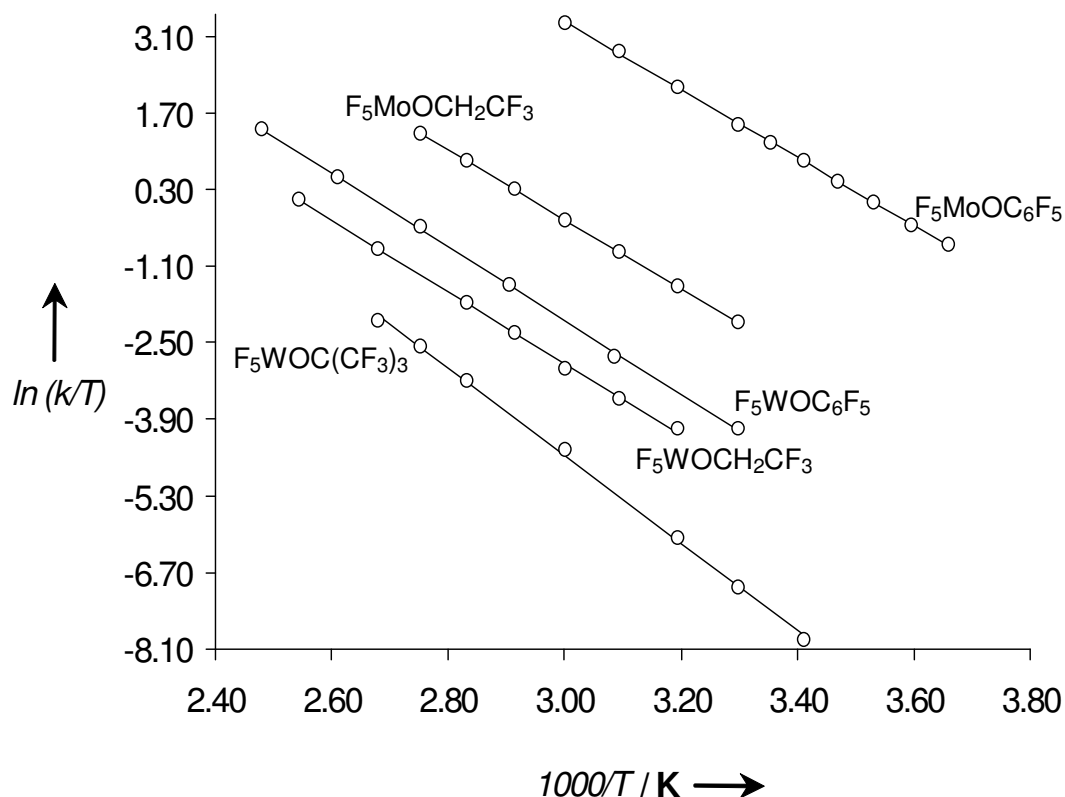
These values can be compared with calculated energies, see table 4 on page 16. Calculated and experimental energy barriers agree fairly well. We must keep in mind that simulations of these dynamic  $^{19}\text{F}$  NMR spectra are not trivial, mainly because there exists a strong temperature dependence of both chemical shifts, especially of the apical fluorine atom, and additionally the high second order character of the  $\text{AB}_4$  systems. The errors of the experimentally determined activation energies can only be guessed. Slight variation of some of the parameters causes changes in the energy values of about  $\pm 0.5 \text{ kcal mol}^{-1}$ .

**Table 5.** Rate constants  $k$  ( $\text{sec}^{-1}$ ) at different temperatures (K) for  $\text{F}_5\text{M}(\text{OCH}_2\text{CF}_3)$ ,  $\text{F}_5\text{M}(\text{OC}_6\text{F}_5)$ ,  $\text{M} = \text{W}, \text{Mo}$ , and  $\text{F}_5\text{W}(\text{OC}(\text{CF}_3)_3)$  obtained by simulations using the Bailar twist (3:3) exchange mode.

$\text{F}_5\text{W}(\text{OCH}_2\text{CF}_3)$		$\text{F}_5\text{W}(\text{OC}_6\text{F}_5)$		$\text{F}_5\text{W}(\text{OC}(\text{CF}_3)_3)$	
$K$	T	$k$	T	$k$	T
5.3	313	5.1	303	0.10	293
9.4	323	20.5	324	0.29	303
16.8	333	80.5	344	0.71	313
33.2	343	250.0	363	3.80	333
58.9	353	645.0	383	14.26	353
170.1	373	1615.0	403	27.57	363
440.8	393			45.62	373

$\text{F}_5\text{Mo}(\text{OCH}_2\text{CF}_3)$		$\text{F}_5\text{Mo}(\text{OC}_6\text{F}_5)$	
$K$	T	$k$	T
35.6	303	135.1	273
71.6	313	196.9	278
138.0	323	299.2	283
256.0	333	444.0	288
460.1	343	656.4	293
796.1	353	926.6	298
1340.2	363	1332.0	303
		2702.7	313
		5405.4	323
		9459.5	333



**Figure 15.** Eyring plot  $\ln\left(\frac{k}{T}\right)$  vs.  $\frac{1000}{T}$  for rate constants obtained by  $^{19}\text{F}$  NMR simulations.

From these energy values obtained it is clearly seen that the molybdenum derivatives have a lower energy barrier for the octahedral-trigonal prismatic rearrangement than the corresponding tungsten ones, as predicted also by the theoretical calculations performed. Furthermore, indeed  $\text{MoF}_6$ ,  $\text{WF}_6$ , and its derivatives are at the edge of structural stability.

The determination of the other activation parameters, like  $\Delta G^\ddagger$  for example, can not be done successfully without introducing a significant error due to the fact that equation (ii)

$$k = \kappa \frac{k_B T}{h} \exp\left(\frac{-\Delta G^\ddagger}{RT}\right) \quad (\text{ii})$$

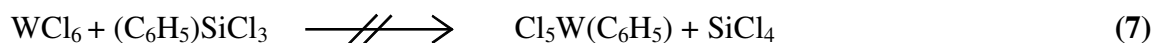
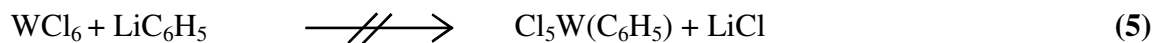
can only be used in full agreement if the so called transmission coefficient ( $\kappa$ ) is exactly known.<sup>[51,53,54,56]</sup> As mentioned before, this coefficient has been used in the literature as 1

or 0.5 for simplicity,<sup>[51,53,54]</sup> but it has been also reported that it could be very small ( $\approx 10^{-7}$ ).<sup>[53]</sup> Therefore any attempt to determine  $\Delta G^\ddagger$  from equation (ii) and furthermore even  $\Delta S^\ddagger$  would rely on the assumption of such value and the results obtained could lead to completely non reliable results. For this reason, no other activation parameters were determined.

## 2.3 MoF<sub>6</sub> and WF<sub>6</sub> derivatives with Alkyl and Phenyl groups as ligands

### 2.3.1 Unsuccessful reactions

Attempts to synthesize and isolate molecules of the type F<sub>6-n</sub>MR<sub>n</sub> (M = Mo or W, R = -C<sub>6</sub>F<sub>5</sub> or -C<sub>6</sub>H<sub>5</sub> and n ≥ 1), which from DFT calculations (see upcoming sections) were predicted as trigonal prismatic, were carried out according to the following reaction schemes:



Reactions (3) to (10) were carried out in different solvents (in some cases even without solvent), in mixtures of solvents, and at different temperatures. In most of the cases an excess of the metal hexafluoride or hexachloride was used in order to obtain only a single substitution. Unfortunately in none of these reactions the desired product or higher

members of the series  $F_{6-n}MR_n$  for  $n \geq 2$  were isolated. All these reactions proved to be unsuccessful and in many cases no reaction occurred between the two species (see experimental section).

A first attempt undertaken with  $WF_6$  and  $Zn(C_6H_5)_2$  (not sublimed) in  $CH_2Cl_2$  according to reaction scheme (3) was monitored using NMR spectroscopy ( $^{19}F$  NMR) from  $-80$  °C to room temperature. No reaction was detected during the whole heating process. Repeating the reaction on a larger scale did not produce different results. After working up the sample (see experimental section), the volatile part was identified as  $WF_6$  and  $CH_2Cl_2$ . The remaining non-volatile black-brown material was very insoluble in  $CH_2Cl_2$ . A  $^{19}F$  NMR of the sample showed no significant new signals. Also no new  $^{19}F$  NMR signals were detected in hexane,  $CCl_4$ , or in diethyl ether.

However, the same reaction carried out in diethyl ether yielded some crystals. Single X-ray diffraction measurements on one of them produced  $[Zn(Et_2O)_2]^{2+} ([F_5WO]^-)_2$  as a structure.  $^{19}F$  NMR of the crystals in acetone showed a doublet (56 ppm, 55 Hz) and a multiplet (30 ppm) corresponding to equatorial and axial fluorine atoms respectively. The formation of the byproduct obtained is attributed to residual water in the solvent and/or in the starting material  $Zn(C_6H_5)_2$  which was not sublimed prior to the synthesis.

The same reaction, but with freshly sublimed diphenyl zinc and freshly distilled  $CH_2Cl_2$  did not produce any kind of hydrolysis byproducts as seen by the  $^{19}F$  NMR, and no reaction was seen between the two reactants.

$MoF_6$  was reacted also with freshly sublimed diphenyl zinc without any solvent. At  $-30$  °C the mixture was gray. Pumping off the  $MoF_6$  excess and adding solvent ( $CH_2Cl_2$ ) to the residue did not give any new signals in the  $^{19}F$  or  $^{13}C$  NMR spectra. No hydrolysis byproducts were detected. The same reaction was carried out in  $CH_2Cl_2$  at room temperature. A sample of the mixture investigated using  $^{19}F$  NMR did not show any reaction between the species.

Reaction scheme (4)

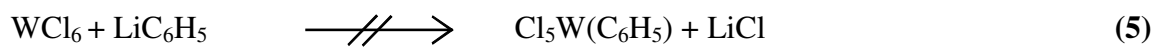


was carried out for both  $\text{WF}_6$  and  $\text{MoF}_6$ . Tungsten hexafluoride, phenyl lithium (not sublimed) and hexane (stored over long period of time over molecular sieve) were reacted at low temperature (see experimental section). A sample of the reaction mixture yielded only one new signal (59 ppm in hexane) in the  $^{19}\text{F}$  NMR. Evacuation of the volatile materials and recondensation of  $\text{CH}_2\text{Cl}_2$  unto the remaining solid gave the same signal (64 ppm in  $\text{CH}_2\text{Cl}_2$ ). This signal is assigned to a hydrolysis byproduct  $(\text{F}_4\text{WO})^{[71]}$  formed from residual water in the solvents which were kept over long periods of time over molecular sieve and to impurities in  $\text{Li}(\text{C}_6\text{H}_5)$  (like  $\text{LiOH}$ ) which was standing in the glove box for a long period of time.

The following procedure was employed to test for residual water in the solvents and/or impurities in phenyl lithium: Phenyl lithium (unsublimed),  $\text{WF}_6$  and freshly distilled hexane were reacted at room temperature. The  $^{19}\text{F}$  NMR spectrum of the sample showed a signal corresponding again to hydrolysis byproduct (in this case due to impurities in the reactant phenyl lithium). Sublimed  $\text{Li}(\text{C}_6\text{H}_5)$ ,  $\text{WF}_6$  and freshly distilled hexane were reacted as before. No hydrolysis byproducts were detected in the  $^{19}\text{F}$  NMR spectrum, neither were there any new signals that could have been attributed to a possible aromatic substitution on  $\text{WF}_6$ .

A similar reaction was tried also with  $\text{MoF}_6$ . After  $\text{MoF}_6$ , diethyl ether (freshly distilled) and  $\text{Li}(\text{C}_6\text{H}_5)$  (sublimed) were reacted at low temperature (see experimental section), a  $^{19}\text{F}$  NMR spectra of the colored (red/orange) product showed two new signals (144 and  $-186$  ppm). A possible reaction was thought to have taken place. Unfortunately the same signals were seen when only  $\text{MoF}_6$  and diethyl ether were stirred together for a couple of hours. Besides these decomposition products of molybdenum hexafluoride and diethyl ether, no NMR signals showing a possible aromatic substitution on molybdenum were detected.

Tungsten hexachloride was reacted with sublimed  $\text{Li}(\text{C}_6\text{H}_5)$  in freshly distilled diethyl ether at room temperature for 24 h. according to reaction scheme (5).



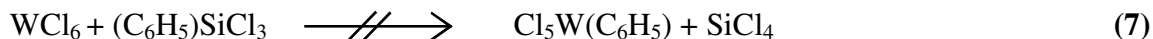
A  $^{13}\text{C}$  NMR of the reaction mixture revealed no significant chemical shift of the aromatic carbons. The PFA tube was sealed and the sample was heated for 24 h at 50 °C. Again,  $^{13}\text{C}$  NMR spectra showed conclusively no reaction between the two species.

Only two attempts to react  $\text{WF}_6$  with pentafluorophenyl-difluoro-borane according to reaction scheme (6) between the two species was carried out.



The main reason was the tedious and unreliable synthesis of  $(\text{C}_6\text{F}_5)\text{BF}_2$  from literature procedures (see experimental section). All attempts to synthesize  $(\text{C}_6\text{F}_5)\text{BF}_2$  prove futile or simply failed as  $\text{C}_6\text{F}_5\text{H}$  was always obtained as the main product. The reaction is achieved by the addition of  $\text{BF}_3$  to a suspension of  $\text{K}[\text{BF}_3(\text{C}_6\text{F}_5)]$  in  $\text{CCl}_3\text{F}$ . After carrying out this reaction the  $^{19}\text{F}$  NMR of the sample always showed  $(\text{C}_6\text{F}_5)\text{BF}_2$  as the main product and in significant amounts as long as  $\text{BF}_3$  was kept in the solution. As soon as the  $\text{BF}_3$  was flushed away from the solution by a stream of argon gas, the main product decomposed completely into  $\text{C}_6\text{F}_5\text{H}$ , and only very small amounts of  $(\text{C}_6\text{F}_5)\text{BF}_2$  were seen to have remained in the solution. The only possible logical explanation is that the argon used could have contained water, but the argon line was checked for leaks and a new  $\text{P}_2\text{O}_{10}$  trap was built and still the desired reaction could not be achieved. Therefore only 2 attempts to react  $(\text{C}_6\text{F}_5)\text{BF}_2$  and  $\text{WF}_6$  were made. Both proved to be unsuccessful.

$\text{WCl}_6$  and previously dried  $(\text{C}_6\text{H}_5)\text{SiCl}_3$  were reacted at room temperature in a mixture of diethyl ether and methylene chloride according to reaction scheme (7).



It is difficult to follow this reaction with NMR spectroscopy. The reason,  $^{13}\text{C}$  and  $^1\text{H}$  NMR's of the reaction mixture showed very unresolved multiplets and no possible detection of any chemical shift is observed. Physical changes in the reaction mixture are definitively observed after stirring the sample for many days at room temperature. The volatile part recovered in a  $-196\text{ °C}$  trap has a light yellow coloration.  $^{13}\text{C}$  NMR of the volatile part showed the educt  $(\text{C}_6\text{H}_5)\text{SiCl}_3$  and traces of a set of new aromatic signals. Attempts to obtain crystals from this liquid were unsuccessful. The remaining dark



red/brown material in the PFA tube was partially soluble in  $\text{CH}_2\text{Cl}_2$ .  $^{13}\text{C}$  and  $^1\text{H}$  NMR spectra of the solution were unreliable for the reasons highlighted above. It was therefore difficult to determine whether a reaction took place or not. Crystallization of this sample afforded yellow needles which were analyzed by X-ray diffraction. After a few scans a pre-analysis of the reflections indicated that the needles contained no aromatic rings bounded to the central atom. The X-ray diffractometer was stopped and the structure was not solved completely.

Some of the remaining crystals were redissolved in  $\text{CH}_2\text{Cl}_2$  and a  $^{13}\text{C}$  NMR of the solution showed no aromatic signals. The rest of the crystals were dissolved in  $\text{CH}_3\text{CH}_2\text{CN}$  and the same  $^{13}\text{C}$  NMR results were obtained. If the tubes with this material are left at room temperature for several days, a black precipitate is formed. That suggests that tungsten is present in the crystals. Due to the fact that neither the X-ray diffraction of the crystals, nor their  $^{13}\text{C}$  NMR spectra revealed aromatic signals, the most logical explanation for these observations (change of color, possible reaction) is that  $\text{WCl}_6$  reacted with diethyl ether giving some decomposition products. No control reaction between  $\text{WCl}_6$  and diethyl ether was carried out to corroborate this explanation. The reaction between tungsten hexachloride and phenyl-trichloro-silane did not produce the desired product(s).

$\text{WF}_6$  and  $\text{MoF}_6$  were reacted with  $(\text{C}_6\text{H}_5)\text{SiF}_3$  according to reaction scheme (8).

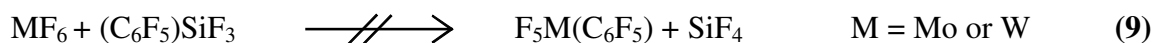


In the case of  $\text{WF}_6$  neither at room temperature, nor at  $40^\circ\text{C}$  for 12 h. could a reaction be detected in the  $^{19}\text{F}$  NMR. Another attempt with  $\text{WF}_6$ ,  $(\text{C}_6\text{H}_5)\text{SiF}_3$ ,  $\text{CH}_2\text{Cl}_2$ , and anhydrous HF was also made. The  $^{19}\text{F}$  NMR of the sample showed no additional signals to those of the starting materials. The two reactants do not react under the given conditions.

For  $\text{MoF}_6$  the same results were obtained. No reaction takes place between the two reactants. If  $\text{CH}_3\text{CN}$  is used as a solvent (which was not freshly distilled, but kept over molecular sieve for a long period of time) a new signal in the  $^{19}\text{F}$  NMR is seen (148

ppm). This signal is assigned to  $[\text{CH}_3\text{CN-MoOF}_4]^{[71]}$  as a hydrolysis byproduct from residual water in the solvent.

Attempts to react  $\text{WF}_6$  or  $\text{MoF}_6$  with  $(\text{C}_6\text{F}_5)\text{SiF}_3$  according to reaction scheme (9) were unsuccessful as well.



For both hexafluorides and in all attempts (see experimental section) no reaction was detected between the two species.

Reaction between  $\text{WF}_6$  and  $(\text{C}_6\text{F}_5)\text{Sn}(\text{CH}_3)_3$  in  $\text{CH}_2\text{Cl}_2$  according to reaction scheme (10) were also performed.



New  $^{19}\text{F}$  NMR signals were observed for this reaction. A possible aromatic substitution on tungsten might have taken place. A doublet at 118.4 ppm (64 Hz), a quintet at 88.5 ppm (64 Hz) and signals corresponding to the aromatic region (-140.1, -155.6, -163.8 ppm) were seen. These signals are very small to be considered as significant. But if any reaction took place and because of the  $\text{AB}_4$  type  $^{19}\text{F}$  NMR spectra seen, the complex should be octahedral. Attempts to crystallize something out of this sample were unsuccessful.

The previous reaction was repeated many times even at 70 °C for 3 days and the relative intensities of the new  $^{19}\text{F}$  NMR signals compared to all other signals present in the spectrum were very negligible. In all of these samples crystallization attempts were unsuccessful. Because of the very small intensities of the new signals, no conclusive statement can be made about the geometry of a possible  $\text{F}_5\text{W}(\text{C}_6\text{F}_5)$  species. Further attempts would be needed in order to arrive to any kind of conclusions.

### 2.3.2 DFT calculations: $-\text{CH}_3$ and $-\text{CF}_3$ groups as ligands

DFT calculations for molecules of the type  $\text{F}_{6-n}\text{MR}_n$  for  $\text{M} = \text{Mo}$  or  $\text{W}$ ,  $\text{R} = -\text{CF}_3$ ,  $-\text{CH}_3$ ,  $-\text{C}_6\text{F}_5$ , and  $-\text{C}_6\text{H}_5$  and  $n \geq 1$  revealed that these complexes should exhibit a trigonal prismatic conformation (distorted in all cases). Theoretical calculations for such molecules were also performed in order to compare their most stable conformation to other calculated molecules of the type  $\text{F}_5\text{MOR}$  (see section 2.2.2) and  $\text{F}_5\text{MSR}$  (see upcoming sections).

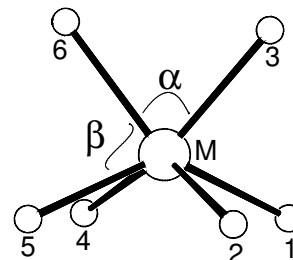
$\text{F}_5\text{Mo}(\text{CH}_3)$ ,  $\text{F}_5\text{Mo}(\text{CF}_3)$ ,  $\text{F}_5\text{W}(\text{CH}_3)$ , and  $\text{F}_5\text{W}(\text{CF}_3)$ , were optimized successfully. All four molecules calculated possess  $\text{C}_s$  symmetry and have a trigonal prismatic (distorted) conformation which is the structure with the minimum energy.

In order to determine which molecules are “more” trigonal prismatic, in other words “less” distorted from an ideal trigonal prism, two approaches were undertaken. A qualitative one (used also by some authors<sup>[12]</sup>) based on comparing the bond lengths and angles obtained for each of the calculated species to those of an hypothetical  $\text{MoF}_6$  or  $\text{WF}_6$  trigonal prismatic structure with  $D_{3h}$  symmetry and see how much they deviate from them. The less these bond lengths and angles deviate from the ideal structures, the “more” trigonal prismatic they would be considered. Of course this is just a qualitative comparison since minor differences in the bond lengths and bond angles can also be attributed to the method and basis set used, but in general since the same method and basis set are used for all molecules the error on the results is systematic.

For this qualitative comparison,  $\alpha$  was chosen for the smallest angles between two hemispheres (3 of them in a trigonal prism),  $\beta$  as the angles within a hemisphere (6 of them in total), and  $\gamma$  as the biggest angles between two hemispheres (6 in total) (see figure 16 in table 6,  $\gamma$  is not shown in the figure). Calculated  $\text{MoF}_6$  and  $\text{WF}_6$  values for both molecules having a  $D_{3h}$  symmetry are listed in table 6.

**Table 6.** DFT calculations on hypothetical MoF<sub>6</sub> and WF<sub>6</sub> trigonal prismatic structures.

Molecule	Geometry* (Symmetry)	M-F (pm)	F-M-F (°)
MoF <sub>6</sub>	Tp, (D <sub>3h</sub> )	186.9	F <sub>6</sub> -W-F <sub>3</sub> ( $\alpha$ ) 78.5
			F <sub>6</sub> -Mo-F <sub>4,5</sub> ( $\beta$ ) 84.2
			F <sub>6</sub> -Mo-F <sub>1,2</sub> ( $\gamma$ ) 134.4
WF <sub>6</sub>	Tp, (D <sub>3h</sub> )	188.0	F <sub>6</sub> -W-F <sub>3</sub> ( $\alpha$ ) 78.4
			F <sub>6</sub> -W-F <sub>4,5</sub> ( $\beta$ ) 84.3
			F <sub>6</sub> -W-F <sub>1,2</sub> ( $\gamma$ ) 134.4

**Figure 16.**

\*Tp = trigonal prismatic

The second approach, a quantitative one, is based on the publications from D. Casanova, et. al, and S. Alvarez, et. al.<sup>[23a, 23b]</sup> Some of the reported aspects which are relevant for the understanding of this quantitative approach are listed and discussed here.

According to the papers mentioned above, to quantify the degree of distortion of a particular molecular structure from an ideal polyhedron one can use *symmetry measures*. This symmetry measure determines the *distance* of a structure from the perfect symmetry of a given point group or from a reference shape. A *symmetry map* (see figure 17) consists of a scatter plot of the symmetry measures relative to two alternative ideal polyhedra. A *symmetry constant* ( $k_{PT}$ ) identifies a distortive route that preserves the minimum distance to two reference symmetries. The minimum distortion angle ( $\theta$ ) directly related to the symmetry constant is unique for each symmetry map. With aid of the symmetry map and symmetry constant the following questions can be address: A) Which is the polyhedra that best describes the geometry of the set of atoms under consideration? B) How far is the real structure from such an ideal geometry?<sup>[23a, 23b]</sup>

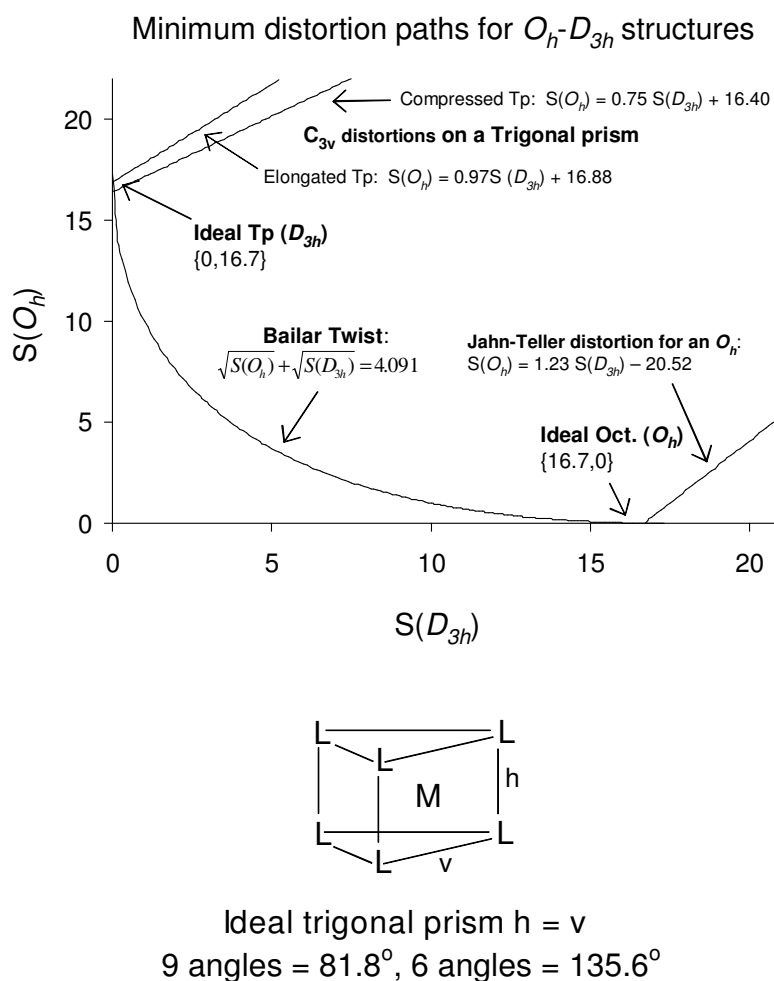


**Figure 17.** Symmetry map for  $O_h$ - $D_{3h}$  species<sup>[23a,23b]</sup> (upper), ideal trigonal prism (lower).

The methodology developed by these authors measures on a quantitative scale the degree of symmetry content in a given structure. If the ideal symmetric object is defined as “G”, then the desired G-symmetry measure,  $S(G)$ , takes values that range from 0 to  $k_{PT}^2$ , where  $k_{PT}$  is the symmetry constant. If  $S(G) = 0$  the structure has the desired G-symmetry and the symmetry measure increases as  $S(G)$  departs from the G-symmetry. Thus when  $S(G) = k_{PT}^2$ , the structure will have no G-symmetry. In the case of the perfect trigonal prismatic structure, “G” would be the trigonal prism with 9 edges of the same length, thus

having 2 equilateral triangles and 3 squares as faces, see figure 17.b. In the case of the perfect octahedral structure “G” would be the octahedron where all bond lengths are equal.<sup>[23a,23b]</sup>

The Bailar twist is the interconversion of an octahedron into a trigonal prism (and vice versa) that produces a symmetry map with the minimum distortion path having a constant  $k_{O_h-D_{3h}} = 4.091$ , where  $S(O_h)$  is the symmetry measure towards the ideal octahedron and  $S(D_{3h})$  towards the ideal trigonal prism.<sup>[23a]</sup> The following relationships hold true for an octahedral-trigonal prismatic interconversion:

$$\sqrt{S(O_h)} + \sqrt{S(D_{3h})} = 4.091 \quad \text{(vii)}$$

$$\arcsin \frac{\sqrt{S(O_h)}}{10} + \arcsin \frac{\sqrt{S(D_{3h})}}{10} = \theta_{O_h-D_{3h}} \quad \text{(viii)}$$

$$k_{O_h-D_{3h}} = \sqrt{S(O_h)} = \sqrt{S(D_{3h})} = 10 \sin \theta_{O_h-D_{3h}} \quad \text{(ix)}$$

$$S(O_h) = 1.23S(D_{3h}) - 20.52 \quad \text{(linear regression for a Jahn-Teller type distortion)} \quad \text{(x)}$$

$$S(O_h) = 0.75S(D_{3h}) + 16.40 \quad \text{(linear regression for a } C_{3v} \text{ distortion, compression)} \quad \text{(xi)}$$

$$S(O_h) = 0.59S(D_{3h}) + 16.74 \quad \text{(linear regression for a } C_{3v} \text{ distortion, truncated trigonal pyramid)} \quad \text{(xii)}$$

$$\Delta(D_{3h}, O_h) \equiv \frac{1}{\theta_{O_h-D_{3h}}} \left[ \arcsin \frac{\sqrt{S(O_h)}}{10} + \arcsin \frac{\sqrt{S(D_{3h})}}{10} \right] - 1 \quad \text{(xiii)}$$

The structure of every hexa-coordinated polyhedron can be identified by its position on the symmetry map presented in figure 17, given by the pair of coordinates  $\{S(D_{3h}), S(O_h)\}$ . The following rules apply:

1. Structures represented by the {16.73,0} point correspond to perfect octahedra.
2. Structures at point {0,16.73} on the symmetry map correspond to ideal trigonal prisms.
3. Other values that obey eqn. (vii) correspond to metaprisms along the Bailar path. Structures with  $S(O_h) < 4.42$  (or  $S(D_{3h}) > 4.42$ ) are closer to the octahedron than to the trigonal prism. Conversely, structures with  $S(O_h) > 4.42$  (or  $S(D_{3h}) < 4.42$ ) are best described as twisted trigonal prisms.
4. Molecular structures with a pair of symmetry measures that do not obey the sum rule of eqn. (vii) (i.e., the sum of square roots is significantly greater than 4.2) correspond to structures that have some distortion other than the Bailar twist, or even the coexistence of a Bailar twist and another distortion. If the sum of square roots is greater than 4.6, then a significant distortion, which is not the Bailar twist, is present.
5. A tetragonal bipyramid characteristic of pure Jahn-Teller distortions of the octahedron is indicated by an  $S(D_{3h})$  value larger than 17 and its  $S(O_h)$  value should obey eqn. (x).
6. Values close to the line represented by eqn. (xi) correspond to a distortion of the type  $C_{3v}$  in which angles larger than  $81.8^\circ$  correspond to a compressed trigonal prism with  $v < h$ , see figure 17 above. If the three upper angles of a trigonal prism are decreased from those of the ideal polyhedron while the lower ones are increased, a truncated trigonal pyramid of  $C_{3v}$  symmetry (represented by eqn. (xii)) results.
7.  $\Delta(D_{3h}, O_h)$  as defined in equation (xiii) is the deviation function that tells how close is the polyhedron studied to the Bailar path.<sup>[23a,23b]</sup>

The program SHAPE<sup>[23c]</sup> was obtained directly from these authors and used to determine the degree of distortion of the complexes being studied here. Since all complexes are calculated with the same method and basis set any deviations and errors from possible experimental values are equivalent for all molecules, therefore a quantitative comparison of the distortions they present would be significant and useful to establish and arrange them as being “more” or “less” trigonal prismatic.

Qualitative approach: Changing a fluorine atom for a  $-\text{CH}_3$  or  $-\text{CF}_3$  group in either  $\text{MoF}_6$  or  $\text{WF}_6$  produces a very small change in the bond lengths between metal and the remaining 5 fluorine atoms (Table 7). In the case of the molybdenum complexes the change in the bond lengths is in average less than + 1.5 pm for the methyl complex and  $\pm 0.6$  pm for the trifluoromethyl one. For the tungsten complexes the deviations are even smaller. These changes are almost negligible and could be attributed to the method and basis set used for these calculations.

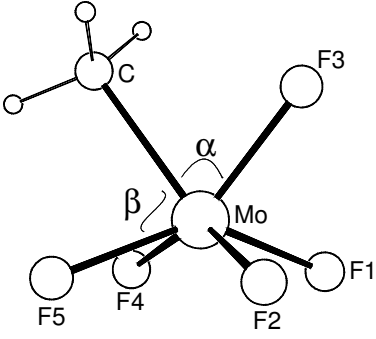
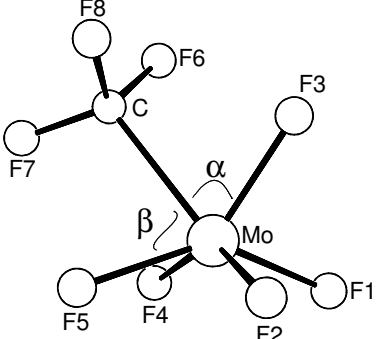
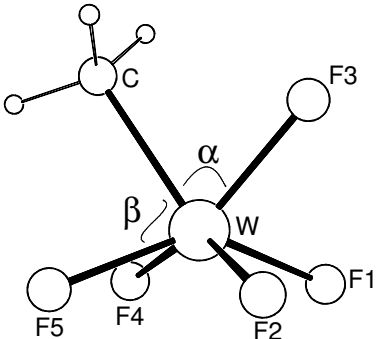
More pronounced changes can be seen in the bond angles, which to some extent could be used as a comparison parameter between the calculated complexes. A decrease in the angles  $\text{C-M-F}_3$  ( $\alpha_1$ ) and  $\text{C-M-F}_{4,5}$  ( $\beta_{1,2}$ ) (Tables 6 and 7 and figures 16, 18-21) for the  $\text{F}_5\text{M}(\text{CH}_3)$  and  $\text{F}_5\text{M}(\text{CF}_3)$  ( $\text{M} = \text{Mo}$  or  $\text{W}$ ) complexes is observed. This was also observed in theoretical calculations on  $\text{Cl}_5\text{W}(\text{CH}_3)$ .<sup>[13]</sup> This reduction of the bond angles can be explained in terms of the steric effect of the  $-\text{CH}_3$  or  $-\text{CF}_3$  groups.<sup>[72]</sup> It is known from the literature that steric requirements of these two groups are greater than those of fluorine and chlorine atoms if they are bonded to other atoms (like oxygen or nitrogen) which produce molecules with small bond lengths, but in molecules with longer bond lengths (like sulfides, phosphines or germanes) the steric requirements are even smaller than those of fluorine or chlorine.<sup>[72]</sup> The latter case happens to be the situation in these complexes, that would explain why a decrease in the angles ( $\alpha_1$  and  $\beta_{1,2}$ ) is observed.

If one compares the bond angles of the  $\text{F}_5\text{W}(\text{CX}_3)$  derivatives to the ideal  $D_{3h}$   $\text{WF}_6$  molecule and the analogous angles of the  $\text{F}_5\text{Mo}(\text{CX}_3)$  complexes to the ideal  $D_{3h}$   $\text{MoF}_6$  molecule, as a general tendency, it is observed that:

- 1)  $\alpha_1$  and  $\beta_{1,2}$  decrease more in the molybdenum derivatives than in the corresponding tungsten ones.
- 2) The decrease in the bond angles is smaller for both  $-\text{CH}_3$  complexes than for the analogous  $-\text{CF}_3$  ones.
- 3) The most pronounced change ( $\approx 9^\circ$ ) in all the derivatives takes place at the angle  $\text{F}_1\text{-M-F}_2$ .



**Table 7.** DFT calculations on molecules of the type  $F_5MR$ ,  $M = Mo$  or  $W$ ,  
 $R = -CH_3$  or  $-CF_3$ .

Molecule <sup>a</sup>	Selected bond distances (pm)	Selected angles (°)
<b><math>F_5Mo(CH_3)</math>, Tp (<math>C_s</math>)</b>		<b>(<math>\alpha</math>) / (<math>\beta</math>) / (<math>\gamma</math>)</b>
	Mo-C 215.0 Mo-F <sub>1,2</sub> 187.8 Mo-F <sub>3</sub> 188.4 Mo-F <sub>4,5</sub> 188.7	C-Mo-F <sub>3</sub> 75.4 C-Mo-F <sub>4,5</sub> 81.5 C-Mo-F <sub>1,2</sub> 128.6 F <sub>3</sub> -Mo-F <sub>1,2</sub> 83.6 F <sub>3</sub> -Mo-F <sub>4,5</sub> 133.1 F <sub>4</sub> -Mo-F <sub>1,2</sub> 79.7 140.7 F <sub>4</sub> -Mo-F <sub>5</sub> 81.3 F <sub>1</sub> -Mo-F <sub>2</sub> 93.9 Twist angle: 0°
<b>Figure 18.</b>		
<b><math>F_5Mo(CF_3)</math>, Tp (<math>C_s</math>)</b>		<b>(<math>\alpha</math>) / (<math>\beta</math>) / (<math>\gamma</math>)</b>
	Mo-C 224.4 Mo-F <sub>1,2</sub> 186.3 Mo-F <sub>3</sub> 187.3 Mo-F <sub>4,5</sub> 187.8	C-Mo-F <sub>3</sub> 74.2 C-Mo-F <sub>4,5</sub> 78.2 C-Mo-F <sub>1,2</sub> 130.6 F <sub>3</sub> -Mo-F <sub>1,2</sub> 86.8 F <sub>3</sub> -Mo-F <sub>4,5</sub> 129.9 F <sub>4</sub> -Mo-F <sub>1,2</sub> 80.6 129.9 F <sub>4</sub> -Mo-F <sub>5</sub> 82.8 F <sub>1</sub> -Mo-F <sub>2</sub> 92.0 Twist angle: 0°
<b>Figure 19.</b>		
<b><math>F_5W(CH_3)</math>, Tp (<math>C_s</math>)</b>		<b>(<math>\alpha</math>) / (<math>\beta</math>) / (<math>\gamma</math>)</b>
	W-C 214.0 W-F <sub>1,2</sub> 189.0 W-F <sub>3</sub> 189.7 W-F <sub>4,5</sub> 189.1	C-W-F <sub>3</sub> 76.0 C-W-F <sub>4,5</sub> 83.5 C-W-F <sub>1,2</sub> 128.1 F <sub>3</sub> -W-F <sub>1,2</sub> 82.2 F <sub>3</sub> -W-F <sub>4,5</sub> 134.3 F <sub>4</sub> -W-F <sub>1,2</sub> 79.1 140.0 F <sub>4</sub> -W-F <sub>5</sub> 81.7 F <sub>1</sub> -W-F <sub>2</sub> 93.9 Twist angle: 0°
<b>Figure 20.</b>		

Continuation table 7.

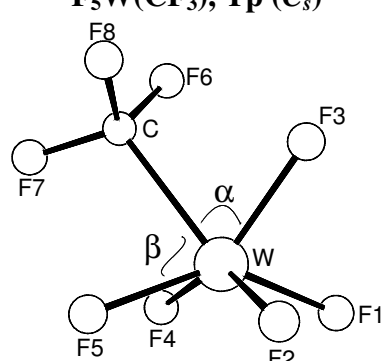
$F_5W(CF_3), Tp (C_s)$		$(\alpha)$	$(\beta)$	$(\gamma)$
	W-C	224.6		
	W-F <sub>1,2</sub>	187.6		
	W-F <sub>3</sub>	188.4		
	W-F <sub>4,5</sub>	188.1		
	C-W-F <sub>3</sub>	74.5		
	C-W-F <sub>4,5</sub>	80.1		
	C-W-F <sub>1,2</sub>		130.2	
	F <sub>3</sub> -W-F <sub>1,2</sub>		85.3	
	F <sub>3</sub> -W-F <sub>4,5</sub>			131.1
	F <sub>4</sub> -W-F <sub>1,2</sub>	80.1		141.1
F <sub>4</sub> -W-F <sub>5</sub>		82.9		
F <sub>1</sub> -W-F <sub>2</sub>		91.7		
Twist angle: 0°				

Figure 21.

<sup>a</sup> Tp = trigonal prismatic.

These general tendencies as a qualitative approach may suggest that both tungsten complexes (methyl and trifluoromethyl) seem to be “less” affected, in other words, less distorted from an ideal  $D_{3h}$  structure than corresponding molybdenum complexes. That would suggest *a priori* that  $F_5W(CH_3)$  and  $F_5W(CF_3)$  seem to be “more” trigonal prismatic than the corresponding molybdenum complexes if one compares them to the hypothetical  $D_{3h}$   $WF_6$  and  $MoF_6$  molecules respectively. In fact that was proven to be the case for  $Mo(CH_3)_6$  and  $W(CH_3)_6$  theoretical calculations<sup>[12]</sup> and experimental<sup>[15,16]</sup> evidence.

Is it possible to justify the fact that the complexes  $F_5M(CH_3)$  ( $M = Mo$  or  $W$ ) appear to be “more” trigonal prismatic than the corresponding  $F_5M(CF_3)$  ones? This question can be answered if the distortion from an ideal  $D_{3h}$  structure is explained in terms of the net charge of the carbon atom in both ligands.<sup>[72-74]</sup>

From previous studies of  $-CF_3$  and  $-CH_3$  derivatives of  $Sn$ ,<sup>[73]</sup>  $Pb$ ,<sup>[73]</sup>  $Ge$ ,<sup>[73,74a,b]</sup> and  $Si$ ,<sup>[75a-d]</sup> it is well known that the carbon atom from  $-CH_3$  carries a small net charge (positive or negative depending on the central atom) while that from  $-CF_3$  carries a very high positive net charge regardless of the central atom.<sup>[72]</sup> This implies that polar and electrostatic effects are highly affected by the net charge of the carbon atom of these two groups. And to some extent this scenario can be correlated here with the distortion of the

complexes from the “ideal” trigonal prism.

A carbon atom possess less electron density (carries a small negative or highly positive net charge) than a fluorine atom which always carries a high negative net charge. Since a fluorine atom will have more electrostatic repulsion with a neighboring fluorine atom than a carbon atom does, one would expect that the former would need more space (bigger angles) to its neighboring fluorine atoms than a carbon atom itself. This might explain why in both  $-\text{CH}_3$  and  $-\text{CF}_3$  derivatives the bond angles  $\text{C}-\text{M}-\text{F}_{3,4,5}$  ( $\alpha_1$  and  $\beta_{1,2}$ ) are smaller than in the hypothetical  $D_{3h}$  molybdenum and tungsten hexafluorides. In other words replacing a fluorine atom by a  $-\text{CH}_3$  or  $-\text{CF}_3$  group in tungsten- or molybdenum hexafluoride reduces the angles to its neighboring fluorine atoms because both carbon atoms have less electron density than the fluorine atom that was replaced.

What happens to either the tungsten or molybdenum complexes if one replaces a  $-\text{CH}_3$  group for  $-\text{CF}_3$  one? That would be the case for  $\text{F}_5\text{W}(\text{CH}_3)$  and  $\text{F}_5\text{W}(\text{CF}_3)$  or  $\text{F}_5\text{Mo}(\text{CH}_3)$  and  $\text{F}_5\text{Mo}(\text{CF}_3)$ . The carbon atom from  $-\text{CF}_3$  is smaller than the carbon atom from  $-\text{CH}_3$  (in the former all electrons have been pulled away),<sup>[72]</sup> consequently it would occupy less space than the methyl carbon. If so, then the  $-\text{CF}_3$  group will have smaller angles to its neighboring fluorine atoms than the  $-\text{CH}_3$  group. This explains why the angles  $\text{C}-\text{M}-\text{F}_3$  ( $\alpha_1$ ) and  $\text{C}-\text{M}-\text{F}_{4,5}$  ( $\beta_{1,2}$ ) for the  $-\text{CF}_3$  complexes are smaller than the analogous  $-\text{CH}_3$  ones in both molybdenum and tungsten molecules, i.e. they have deviated more from the ideal  $D_{3h}$  hexafluoride. That would suggest that the trifluoromethyl complexes are “more” distorted relative to this ideal structure than the methyl ones. Therefore they would be considered “less” trigonal prismatic than the corresponding methyl derivatives.

A SHAPE<sup>[23c]</sup> analysis (see table 8 and figure 22) on all four molecules mentioned before revealed the following aspects: The departure from the Bailar twist rearrangement path is in general around 15% ( $\Delta(D_{3h}, O_h) \approx 0.15$ ). The sum of square roots is greater than 4.6, therefore the complexes have a distortion which is not caused by the Bailar twist, rather it is a  $C_{3v}$  distortion in which the bonds and bond angles were affected resulting in a truncated trigonal pyramid (Figure 22).

For  $F_5Mo(CH_3)$  the point  $\{S(D_{3h}), S(O_h)\}$  is closer to  $\{0,16.7\}$  (an ideal trigonal prism) than for  $F_5Mo(CF_3)$ , therefore the former is more trigonal prismatic. For the tungsten complexes no conclusive comparison can be made, the difference in  $S(D_{3h})$  and  $S(O_h)$  is not significant.<sup>[23c]</sup>  $F_5Mo(CH_3)$  is more trigonal prismatic than  $F_5W(CF_3)$ , i.e the point  $\{S(D_{3h}),S(O_h)\}$  is closer to  $\{0,16\}$  in the former.  $F_5W(CF_3)$  might be more trigonal prismatic than  $F_5Mo(CF_3)$ , even though the difference in the values  $S(O_h)$  and  $S(D_{3h})$  is too small to make a conclusive statement.

**Table 8.** SHAPE<sup>[23c]</sup> analysis for complexes of the type  $F_5MR$  ( $M = Mo$  or  $W$ ;  $R = -CF_3$  or  $-CH_3$ ).

Complex	$S(D_{3h})$	$S(O_h)$	$\Delta(D_{3h},O_h)$	$\sqrt{S(D_{3h})} + \sqrt{S(O_h)}$
$F_5Mo(CH_3)$	0.361	16.891	0.147	4.711
$F_5W(CF_3)$	0.401	16.925	0.156	4.748
$F_5W(CH_3)$	0.418	16.924	0.159	4.760
$F_5Mo(CF_3)$	0.433	16.963	0.163	4.776

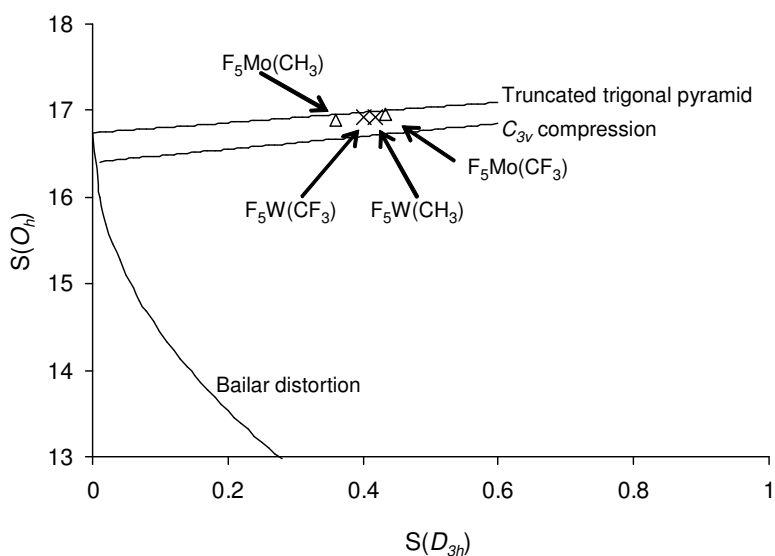


**Figure 22.** Symmetry map analysis for molecules of the type  $F_5MR$ ,  $M = Mo$  or  $W$ ,  $R = -CH_3$ , or  $-CF_3$ .

Based on the qualitative and quantitative analysis made, a tentative series in which complexes are arranged as being less distorted (“more” trigonal prismatic) towards an ideal  $D_{3h}$  structure from left to right and from top to bottom can be presented, see table 9.

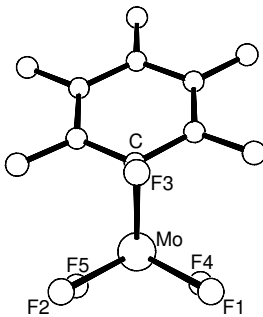
**Table 9.**  $WF_6$  and  $MoF_6$  trigonal prismatic derivatives arranged according to their distortion (left to right, top to bottom) towards an ideal  $D_{3h}$  structure.

	Less distorted	More distorted
	$F_5W(CH_3)$	$F_5Mo(CH_3)$
More distorted	$F_5W(CF_3)$	$F_5Mo(CF_3)$

### 2.3.3 DFT calculations: $-C_6H_5$ and $-C_6F_5$ groups as ligands

Calculations using bigger ligands than  $-CH_3$  and  $-CF_3$  were also performed to see if an increase in the ligand size would affect the ground state conformation of the compounds of interest. Both single substituted  $-C_6F_5$  (tungsten and molybdenum) complexes (see table 10) are trigonal prismatic (distorted), on the contrary the  $-C_6H_5$  ones (Table 12, discussed later) are not.

**Table 10.** Results of DFT calculations on molecules of the type  $F_5M(C_6F_5)$ ,  $M = Mo$  or  $W$ .

Molecule <sup>a</sup>	Selected bond distances (pm)	Selected angles (°)
$F_5Mo(C_6F_5)$ , Tp (distorted)		( $\alpha$ ) / ( $\beta$ ) / ( $\gamma$ )
	Mo-C 212.8	C-Mo-F <sub>3</sub> 77.1
	Mo-F <sub>1</sub> 187.3	C-Mo-F <sub>4,5</sub> 84.1, 84.5
	Mo-F <sub>2</sub> 187.1	C-Mo-F <sub>1,2</sub> 131.6, 129.3
	Mo-F <sub>3</sub> 189.3	F <sub>4</sub> -Mo-F <sub>1,2,3</sub> 79.0 138.1, 133.7
	Mo-F <sub>4</sub> 188.2	F <sub>5</sub> -Mo-F <sub>2,1,3</sub> 78.9 136.5, 136.5
	Mo-F <sub>5</sub> 188.0	F <sub>3</sub> -Mo-F <sub>1,2</sub> 82.4, 83.4
		F <sub>4</sub> -Mo-F <sub>5</sub> 81.6
		F <sub>1</sub> -Mo-F <sub>2</sub> 90.3
		Twist angle: 2°

**Figure 23.**

front face (F1,F2,F3)

back face (F4,F5,C)

Continuation table 10.

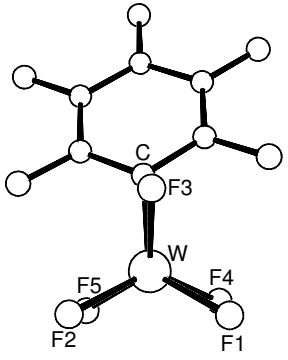
$F_5W(C_6F_5)$ , Tp (distorted)			$(\alpha) / (\beta) / (\gamma)$		
	Mo-C	214.2	C-Mo-F <sub>3</sub>	77.3	
	Mo-F <sub>1</sub>	188.6	C-Mo-F <sub>4,5</sub>	85.0, 84.9	
	Mo-F <sub>2</sub>	188.2	C-Mo-F <sub>1,2</sub>		133.8, 126.8
	Mo-F <sub>3</sub>	190.0	F <sub>4</sub> -Mo-F <sub>1,2,3</sub>	78.7	140.3, 131.6
	Mo-F <sub>4</sub>	188.8	F <sub>5</sub> -Mo-F <sub>2,1,3</sub>	78.7	133.8, 139.3
	Mo-F <sub>5</sub>	188.5	F <sub>3</sub> -Mo-F <sub>1,2</sub>	81.9, 83.2	
			F <sub>4</sub> -Mo-F <sub>5</sub>	81.8 /	
			F <sub>1</sub> -Mo-F <sub>2</sub>	90.5	

Figure 24.

front face (F1,F2,F3)

back face (F4,F5,C)

Twist angle: 5.3°

<sup>a</sup> Tp = trigonal prismatic

What is the extent of distortion on the molecules upon introduction of a  $-C_6F_5$  group? Qualitatively differences in the bond lengths and bond angles are difficult to compare in order to determine how distorted each molecule is. From here on, any kind of distortion presented by the studied complexes will be based solely on the output of the program SHAPE.<sup>[23c]</sup>

A SHAPE analysis of the two complexes (see table 11) shows the following facts: The sum of square roots ( $\sqrt{S(D_{3h})} + \sqrt{S(O_h)}$ ) is greater than 4.2 but not greater than 4.6, so both structures are trigonal prisms which are distorted by a Bailar twist and a combination of another distortion. The other most probable distortion that they present is a Jahn-Teller type,<sup>[23b]</sup> which in both molecules is almost of the same magnitude (the sum of square roots are almost similar). In other words, the structures can be described as having some bond stretch distortion acting on a twisted trigonal prism.<sup>[23b]</sup> In general,  $F_5Mo(C_6F_5)$  is less Bailar distorted, i.e. is more trigonal prismatic, than  $F_5W(C_6F_5)$  because  $\{0.336, 16.068\}$  is closer to  $\{0, 16.7\}$  than  $\{0.476, 14.5\}$  respectively.

**Table 11.** SHAPE<sup>[23c]</sup> analysis for complexes of the type F<sub>5</sub>M(C<sub>6</sub>F<sub>5</sub>) (M = Mo or W).

Complex	S( <i>D</i> <sub>3h</sub> )	S( <i>O</i> <sub>h</sub> )	Δ( <i>D</i> <sub>3h</sub> , <i>O</i> <sub>h</sub> )	$\sqrt{S(D_{3h})} + \sqrt{S(O_h)}$
F <sub>5</sub> Mo(C <sub>6</sub> F <sub>5</sub> )	0.336	16.068	0.116	4.588
F <sub>5</sub> W(C <sub>6</sub> F <sub>5</sub> )	0.476	14.510	0.091	4.499

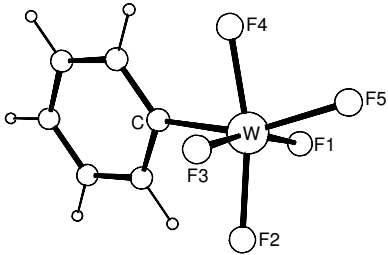
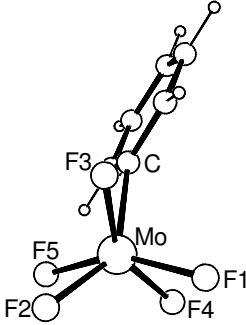
The trigonal twist angle (0° for a trigonal prism, 60° for an octahedron) has been used before as a parameter to determine the distortion of the molecule towards an ideal prism.<sup>[76a-d]</sup>

From the SHAPE analysis which was carried out, it can be seen that the trigonal twist angle can not account solely for the distortion of a structure. For example, F<sub>5</sub>Mo(C<sub>6</sub>F<sub>5</sub>) has a twist angle of 2° whereas F<sub>5</sub>Mo(CH<sub>3</sub>) has a value of 0° (due to the C<sub>s</sub> symmetry), still the later is not a perfect trigonal prism (S(*O*<sub>h</sub>) ≠ 16.7) and has a distortion of the type C<sub>3v</sub> and not of the Bailar type. That happens to be the case also for F<sub>5</sub>Mo(C<sub>6</sub>F<sub>5</sub>) (twist angle 5.3°) and F<sub>5</sub>Mo(CH<sub>3</sub>) (twist angle 0°). The twist angle can only be used to compare distortions which are mainly produced by the Bailar twist (and to some extent combined with an extra small Jahn-Teller type distortion). In any other case of trigonal prismatic distortion, like C<sub>3v</sub> for example, it is meaningless to do this kind of comparison.

Both F<sub>5</sub>Mo(C<sub>6</sub>F<sub>5</sub>) and F<sub>5</sub>W(C<sub>6</sub>F<sub>5</sub>) have clearly a Bailar distortion, F<sub>5</sub>Mo(C<sub>6</sub>F<sub>5</sub>) has a twist angle of 2° and F<sub>5</sub>W(C<sub>6</sub>F<sub>5</sub>) of 5.3°. So F<sub>5</sub>Mo(C<sub>6</sub>F<sub>5</sub>) is less distorted on the Bailar pathway towards an ideal trigonal prism than F<sub>5</sub>W(C<sub>6</sub>F<sub>5</sub>). That is also confirmed by the fact that the point {S(*D*<sub>3h</sub>),S(*O*<sub>h</sub>)} is closer to the ideal *D*<sub>3h</sub> structure in the former.

Unlike the single substituted –C<sub>6</sub>F<sub>5</sub> derivatives, the –C<sub>6</sub>H<sub>5</sub> group bearing molecules (see table 12) are not necessarily trigonal prismatic. For F<sub>5</sub>W(C<sub>6</sub>H<sub>5</sub>) the minimum energy structure obtained is definitively more octahedral than trigonal prismatic. That can be easily seen by the angles which are closer to 180° and 90° (Table 12) and was corroborated with the SHAPE<sup>[23]</sup> analysis: S(*D*<sub>3h</sub>) = 7.362, S(*O*<sub>h</sub>) = 3.064, Δ ≈ 7%, see table 13. So F<sub>5</sub>W(C<sub>6</sub>H<sub>5</sub>) can be better described as an octahedron which is twisted (Bailar type) with some little Jahn-Teller type distortion (sum of square roots ≈ 4.4).

**Table 12.** Results of DFT calculations on molecules of the type  $F_5M(C_6H_5)$ ,  $M = W$  or  $Mo$ .

Molecule <sup>a</sup>	Selected bond distances (pm)		Selected angles (°)	
<b><math>F_5W(C_6H_5)</math>, Oct. (distorted)</b>			90°	/ 180°
			C–Mo–F <sub>1,3</sub>	86.3, 101.0
			C–Mo–F <sub>2,4</sub>	93.6, 80.3
	Mo–C	210.9	C–Mo–F <sub>5</sub>	153.7
	Mo–F <sub>1</sub>	189.4	F <sub>1</sub> –Mo–F <sub>2,4</sub>	84.3, 107.5
	Mo–F <sub>2</sub>	189.0	F <sub>1</sub> –Mo–F <sub>3</sub>	164.7
	Mo–F <sub>3</sub>	188.6	F <sub>1</sub> –Mo–F <sub>5</sub>	82.7
	Mo–F <sub>4</sub>	190.1	F <sub>2</sub> –Mo–F <sub>4</sub>	166.1
	Mo–F <sub>5</sub>	191.3	F <sub>3</sub> –Mo–F <sub>2,4</sub>	81.8, 87.1
			F <sub>3</sub> –Mo–F <sub>5</sub>	95.7
			F <sub>5</sub> –Mo–F <sub>2,4</sub>	108.9, 80.4
<b><math>F_5Mo(C_6H_5)</math> Tp (very distorted)</b>			( $\alpha$ ) / ( $\beta$ ) / ( $\gamma$ )	
	Mo–C	211.7	C–Mo–F <sub>3</sub>	78.4
	Mo–F <sub>1</sub>	188.5	C–Mo–F <sub>4,5</sub>	88.3, 82,4
	Mo–F <sub>2</sub>	188.6	C–Mo–F <sub>1,2</sub>	113.3, 142.0
	Mo–F <sub>4</sub>	188.7	F <sub>4</sub> –Mo–F <sub>1,2,3</sub>	79.2, 121.7, 150.9
	Mo–F <sub>3</sub>	189.3	F <sub>5</sub> –Mo–F <sub>2,3,1</sub>	80.2, 121.5, 154.6
	Mo–F <sub>5</sub>	189.4	F <sub>3</sub> –Mo–F <sub>1,2</sub>	82.4
			F <sub>4</sub> –Mo–F <sub>5</sub>	81.5
			F <sub>1</sub> –Mo–F <sub>2</sub>	96.1
			Twist angle:	18.9°

<sup>a</sup> Oct. = octahedral; Tp = trigonal prismatic.**Table 13.** SHAPE<sup>[23c]</sup> analysis for complexes of the type  $F_5M(C_6H_5)$  ( $M = Mo$  or  $W$ ).

Complex	$S(D_{3h})$	$S(O_h)$	$\Delta(D_{3h}, O_h)$	$\sqrt{S(D_{3h})} + \sqrt{S(O_h)}$
$F_5Mo(C_6H_5)$	2.575	8.006	0.063	4.434
$F_5W(C_6H_5)$	7.362	3.064	0.069	4.464



On the other hand,  $F_5Mo(C_6H_5)$  can be interpreted (qualitative) as two possible structures either as a very distorted trigonal prism (like shown in figure 26 in table 12) or as a bicapped tetrahedron, the former being the most appropriate one. The choice of such geometry (distorted trigonal prism) is based solely on the results provided by the SHAPE analysis: the geometry of  $F_5Mo(C_6H_5)$  lies very close ( $\Delta \approx 6\%$ ) to the minimum distortion path produced by the Bailar twist. The molecule has mainly this kind of distortion ( $4.2 < \text{sum of square roots} < 4.6$ ) and not a distortion like the bicapped tetrahedron. Furthermore,  $F_5Mo(C_6H_5)$  is more trigonal prismatic than octahedral,  $S(D_{3h}) < 4.42$  or  $S(O_h) > 4.42$ . So  $F_5Mo(C_6H_5)$  can be described as a trigonal prism which is twisted (Bailar type) with some little Jahn-Teller type distortion (sum of square roots  $\approx 4.5$ ).

For reasons that are still unclear, both single substituted  $-C_6H_5$  molybdenum and tungsten complexes are more Bailar distorted from an ideal trigonal prismatic structure than the corresponding  $-C_6F_5$  compounds, and  $F_5W(C_6H_5)$  even prefers an octahedral conformation rather than a trigonal prismatic. Also the phenyl- and pentafluorophenyl-molybdenum complexes are less Bailar distorted from an ideal trigonal prism than the corresponding tungsten ones. That is not the case for  $W(CH_3)_6$  and  $Mo(CH_3)_6$  in which the former happens to be less distorted.<sup>[15,16]</sup>

So, in general it can be postulated from this shape analysis that in the case of smaller groups like  $-CX_3$  ( $X = H$  or  $F$ ) both tungsten and molybdenum complexes exhibit a  $C_{3v}$  type of distortion which in the molybdenum ones is more pronounced. On the other hand, for the  $-C_6X_5$  ( $X = H$  or  $F$ ) complexes, the main distortion is of the type Bailar (with some Jahn-Teller type of distortion) and the molybdenum derivatives are less distorted towards an ideal  $D_{3h}$  structure than the tungsten ones.

A possible explanation for these findings is the following: If one compares the bond lengths of the  $-CX_3$  derivatives with those of the corresponding  $-C_6X_5$  ones, it is seen that with the basis set and method used, there is almost no significant difference between them. So if the bond lengths remain almost the same, the most logical explanation for such an observation is the steric requirement of the  $-C_6X_5$  groups. In other words, in

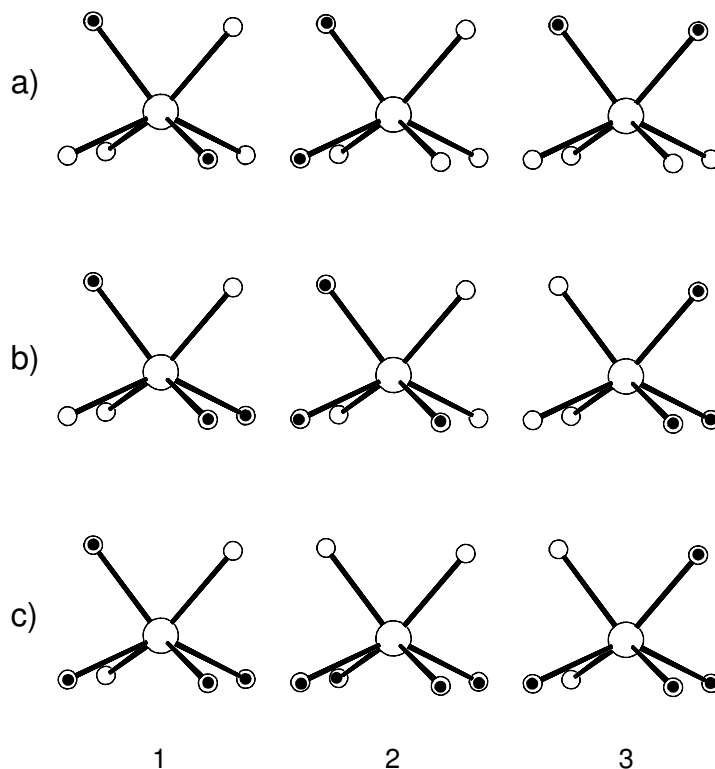
order for the  $-C_6X_5$  group to “fit” in the molecule with almost the same bond lengths as the  $-CX_3$  derivatives, the triangular faces of the trigonal prism would need to be twisted, i.e. a much pronounced Bailar twist would be expected. That indeed suggests that smaller ligands like  $-CX_3$  for example will induce mainly a  $C_{3v}$  type distortion, while bigger ones like  $-C_6X_5$  will present mainly a Bailar type distortion.

For all other higher members of the series  $F_{6-n}Mo(C_6F_5)_n$  ( $n = 2 - 4$ ), a distorted (mainly of the Bailar type) trigonal prismatic conformation, was found to be the structure with the minimum energy (see tables 14 and 15). Even with a fourth substitution on molybdenum the structure with the minimum energy could still be considered as a distorted trigonal prism.

For the  $F_4Mo(C_6F_5)_2$  molecules all three possible isomeric structures (Figure 27.a) were calculated. For a third substitution only two of the three possible isomeric structures were calculated (Figure 27.b, isomers 1 and 2) because the amount of time needed for each calculation is enormous. Introducing a fourth  $-C_6F_5$  ligand to the molecule increases the calculation time so much that in this case only one isomer, which was presumed to have the lowest energy (based on steric requirements of the ligands), was calculated (Figure 27.c, isomer 1).

For the single substituted tungsten derivatives the computational time needed was somehow greater than for the molybdenum ones, therefore no higher members of the series  $F_{6-n}W(C_6F_5)_n$  ( $n \geq 2$ ) were calculated.

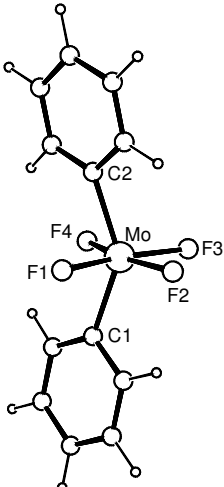
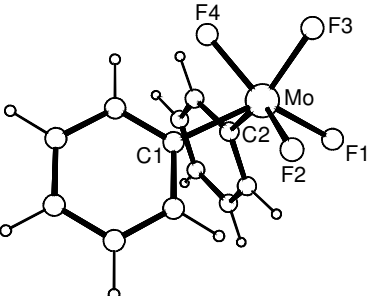
Surprisingly,  $F_4Mo(C_6H_5)_2$  was optimized successfully with two different geometries, none of them being a transition state and both being energy minima, see table 14. If the starting molecule is set as a *trans*-octahedral derivative the optimization for an energy minimum gives a molecule which is very distorted, but still octahedral (Figure 28 in table 14). But if the starting molecule is set as *cis*-octahedral derivative then the end result is an almost perfect trigonal prismatic structure (Figure 29 in table 14).



**Figure 27.** Possible isomers for a) double, b) triple, and c) quadruple substitution on a trigonal prism, arranged in order of increasing energy:  $E_1 < E_2 < E_3$ .

In fact, M. Kaupp<sup>[13]</sup> performed calculations on  $\text{Cl}_4\text{W}(\text{CH}_3)_2$  species and found a *trans*-octahedral complex which was around  $10 \text{ kJ mol}^{-1}$  ( $2.4 \text{ kcal mol}^{-1}$ ) lower in energy than a structure that was neither octahedral, nor trigonal prismatic (with  $C_2$  symmetry) but closer to a trigonal prism (with  $C_{2v}$  symmetry) than to the *cis*-octahedral complex ( $C_s$ ). He also proposed that the interconversion in this complex can be achieved by rotation of the face  $-(\text{CH}_3)_2\text{Cl}$  (which happens to be the Bailar twist.<sup>[19]</sup>). He even suggests the fact that the energy between an octahedral and prismatic structure has essentially vanished in these species so that the system can be considered as “highly fluxional”.

**Table 14.** Results of DFT calculations on  $F_4Mo(C_6H_5)_2$ .

Molecule <sup>a</sup>	Selected bond distances (pm)	Selected angles (°)
<b><i>trans</i>-<math>F_4Mo(C_6H_5)_2</math>, Oct. (distorted)</b>		
	Mo-C <sub>1,2</sub> 209.2 Mo-F <sub>1</sub> 191.3 Mo-F <sub>2</sub> 191.9 Mo-F <sub>3</sub> 189.1 Mo-F <sub>4</sub> 195.4	C <sub>1</sub> -Mo-C <sub>2</sub> 142.2 F <sub>1</sub> -Mo-F <sub>3,2</sub> 163.3, 82.2 F <sub>4</sub> -Mo-F <sub>2,3</sub> 164.9, 84.4 C <sub>1</sub> -Mo-F <sub>1,2</sub> 82.9, 106.4 C <sub>2</sub> -Mo-F <sub>1,2</sub> 82.8, 106.3
<b><math>F_4Mo(C_6H_5)_2</math>, Tp (<math>\approx C_s</math>) (isomer 2)</b>		( $\alpha$ ) / ( $\beta$ ) / ( $\gamma$ )
	Mo-C <sub>1</sub> 215.0 Mo-C <sub>2</sub> 214.9 Mo-F <sub>1,2</sub> 189.0 Mo-F <sub>3</sub> 189.6 Mo-F <sub>4</sub> 190.6	C <sub>1</sub> -Mo-C <sub>2</sub> 82.1 C <sub>1,2</sub> -Mo-F <sub>4</sub> 80.7, 80.8 C <sub>1</sub> -Mo-F <sub>2,1</sub> 78.0, 129.9 C <sub>2</sub> -Mo-F <sub>1,2</sub> 78.0, 129.9 F <sub>3</sub> -Mo-F <sub>4</sub> 78.7 F <sub>4</sub> -Mo-F <sub>1,2</sub> 138.8, 138.7 F <sub>3</sub> -Mo-C <sub>1,2</sub> 133.8, 133.7 F <sub>3</sub> -Mo-F <sub>1,2</sub> 91.1, 91.2 F <sub>1</sub> -Mo-F <sub>2</sub> 80.5
		Twist angle: 0.1°

<sup>a</sup> Oct = octahedral, Tp = trigonal prismatic.

In the calculations done in this thesis the *trans*-octahedral complex (Figure 28 in table 14) is only  $\approx 6$  kcal mol<sup>-1</sup> (with zero-point vibrational energy correction) lower in energy than the trigonal prismatic ( $\approx C_s$ , isomer 2) one, see figure 29 in table 14. These

findings are very interesting because any attempt to synthesize and isolate  $F_4W(C_6H_5)_2$  could produce either of the two possible structures, or even a structure with an intermediate geometry. Just like M. Kaupp described it for the  $Cl_{6-n}W(CH_3)_n$  complexes, the energy for such a rearrangement has vanished in this species, such that it could be considered as highly fluxional.

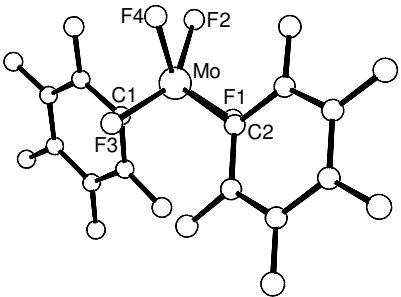
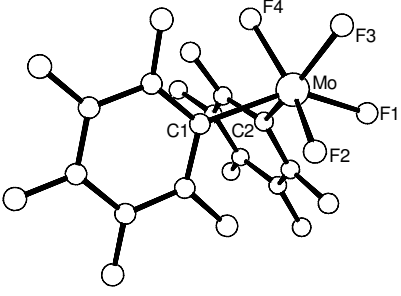
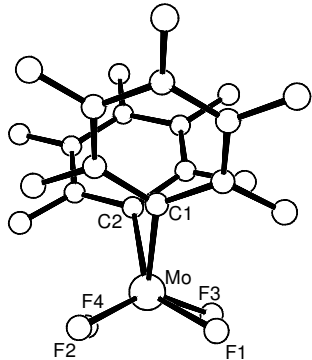
However, none of the two possible isomers (*cis* and *trans*) for a double substituted  $-C_6F_5$  octahedral derivative produces an octahedral structure as the conformation with the minimum energy. Instead, all three trigonal prismatic isomers are obtained, see figures 30-32 in table 15. Isomer 1 is barely lower in energy than isomer 2 ( $\approx 3.2 \text{ kcal mol}^{-1}$ ) and isomer 3 is  $5.5 \text{ kcal mol}^{-1}$  higher than isomer 2. So isomer 1 and 2 seem to be closer in energy than isomer 2 and 3. In fact K. Seppelt, et. al.<sup>[16]</sup> were able to crystallize  $(CH_3)_4W(OCH_3)_2$  as a trigonal prismatic structure (isomer 2) which indeed suggests that such a low energy barrier could afford any of the desired isomers. That could be also the case for the  $-C_6F_5$  derivatives.

These findings about the phenyl- single and double substituted tungsten and molybdenum complexes can still not be explained. No logical explanation has been found for the facts that:  $F_5W(C_6H_5)$  is an octahedron (Bailar distorted) whereas  $F_5W(C_6F_5)$  is a trigonal prism (also Bailar distorted),  $F_5Mo(C_6H_5)$  is a very Bailar distorted trigonal prism but  $F_5Mo(C_6F_5)$  adopts an almost perfect trigonal prismatic structure. *Trans*- $F_4Mo(C_6H_5)_2$  prefers the octahedral environment whereas  $F_4Mo(C_6F_5)_2$  adopts always a trigonal prismatic structure regardless of the position of the ligands. Only experimental evidence will be decisive for these interpretations.

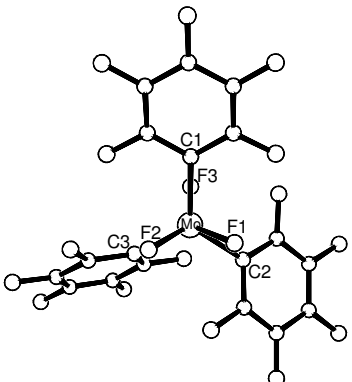
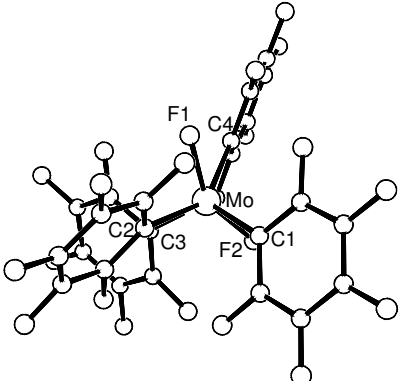
The only things that can be assured about these findings are that:

1.  $-C_6H_5$  as a ligand produces more Bailar distortion from a trigonal prismatic structure on both molybdenum and tungsten than  $-C_6F_5$  does.
2. Tungsten substituted  $-C_6H_5$  and  $-C_6F_5$  complexes have more Bailar distortion from an ideal  $D_{3h}$  structure than the corresponding molybdenum ones.

**Table 15.** Results of DFT calculations on molecules of the type  $F_{6-n}Mo(C_6F_5)_n$ ,  $n = 2-4$ .

Molecule <sup>a</sup>	Selected bond distances (pm)	Selected angles (°)
<b><math>F_4Mo(C_6F_5)_2</math> (Isomer 1), Tp distorted (<math>\approx C_2</math>)</b>		
	Mo–C <sub>1</sub> 212.3 Mo–C <sub>2</sub> 212.2 Mo–F <sub>2,4</sub> 188.3 Mo–F <sub>1,3</sub> 190.4	( $\alpha$ ) / ( $\beta$ ) / ( $\gamma$ ) C <sub>1</sub> –Mo–C <sub>2</sub> 134.3 C <sub>1</sub> –Mo–F <sub>2,4</sub> 90.4, 125.8 C <sub>2</sub> –Mo–F <sub>4,2</sub> 90.6, 125.9 C <sub>1</sub> –Mo–F <sub>3,1</sub> 77.9, 82.1 C <sub>2</sub> –Mo–F <sub>1,3</sub> 78.0, 82.1 F <sub>2</sub> –Mo–F <sub>1,3</sub> 81.4, 146.1 F <sub>4</sub> –Mo–F <sub>3,1</sub> 81.5, 146.3 F <sub>4</sub> –Mo–F <sub>2</sub> 79.9 F <sub>1</sub> –Mo–F <sub>3</sub> 127.1 Twist angle: 19.8°
<b>Figure 30.</b> front face (C2,F3,F4) back face (F1,C1,F2)		
<b><math>F_4Mo(C_6F_5)_2</math> (Isomer 2), Tp distorted</b>		
	Mo–C <sub>1</sub> 215.1 Mo–C <sub>2</sub> 218.1 Mo–F <sub>1</sub> 188.3 Mo–F <sub>2</sub> 188.2 Mo–F <sub>3</sub> 189.4 Mo–F <sub>4</sub> 186.4	( $\alpha$ ) / ( $\beta$ ) / ( $\gamma$ ) C <sub>1</sub> –Mo–C <sub>2</sub> 81.5 C <sub>1,2</sub> –Mo–F <sub>4</sub> 84.2, 83.9 C <sub>1</sub> –Mo–F <sub>2,1</sub> 78.7, 143.6 C <sub>2</sub> –Mo–F <sub>1,2</sub> 78.5, 118.6 F <sub>3</sub> –Mo–F <sub>4</sub> 79.4 F <sub>4</sub> –Mo–F <sub>1,2</sub> 123.2, 149.8 F <sub>3</sub> –Mo–C <sub>1,2</sub> 125.4, 145.9 F <sub>3</sub> –Mo–F <sub>1,2</sub> 86.2, 89.5 F <sub>1</sub> –Mo–F <sub>2</sub> 84.5 Twist angle: 15.1°
<b>Figure 31.</b>		
<b><math>F_4Mo(C_6F_5)_2</math> (Isomer 3), Tp distorted</b>		
	Mo–C <sub>1,2</sub> 215.9 Mo–F <sub>1,4</sub> 189.0 Mo–F <sub>2,3</sub> 187.3	( $\alpha$ ) / ( $\beta$ ) / ( $\gamma$ ) C <sub>1</sub> –Mo–C <sub>2</sub> 76.2 C <sub>1</sub> –Mo–F <sub>1,2</sub> 80.8, 85.3 C <sub>2</sub> –Mo–F <sub>4,3</sub> 80.9, 85.4 C <sub>1</sub> –Mo–F <sub>3,4</sub> 123.8, 139.3 C <sub>2</sub> –Mo–F <sub>2,1</sub> 123.9, 139.3 F <sub>1</sub> –Mo–F <sub>3,4</sub> 80.3, 135.3 F <sub>2</sub> –Mo–F <sub>4,3</sub> 80.3, 144.8 F <sub>1</sub> –Mo–F <sub>2</sub> 86.4 F <sub>3</sub> –Mo–F <sub>4</sub> 86.6 Twist angle: 12.1°
<b>Figure 32.</b> front face (F1,F2,C1) back face (F3,F4,C2)		

Continuation table 15.

<b>F<sub>3</sub>Mo(C<sub>6</sub>F<sub>5</sub>)<sub>3</sub> (Isomer 1), Tp distorted</b>		( $\alpha$ ) / ( $\beta$ ) / ( $\gamma$ )
	Mo–C <sub>1</sub> 211.9 Mo–C <sub>2</sub> 211.5 Mo–C <sub>3</sub> 220.1 Mo–F <sub>1</sub> 192.6 Mo–F <sub>2</sub> 188.0 Mo–F <sub>3</sub> 190.3	C <sub>1</sub> –Mo–F <sub>3,1,2</sub> 79.2, 84.9, 91.3 C <sub>2</sub> –Mo–F <sub>1,3,2</sub> 76.4, 83.4, 128.2 C <sub>3</sub> –Mo–F <sub>2,3,1</sub> 78.0, 78.0, 140.7 C <sub>1</sub> –Mo–C <sub>2,3</sub> 129.4, 126.36 F <sub>1,2</sub> –Mo–F <sub>3</sub> 136.9, 142.1 C <sub>2</sub> –Mo–C <sub>3</sub> 95.1 F <sub>1</sub> –Mo–F <sub>2</sub> 77.4
<b>Figure 33.</b> front face (F <sub>1</sub> ,F <sub>2</sub> ,C <sub>1</sub> ) back face (C <sub>2</sub> ,C <sub>3</sub> ,F <sub>3</sub> )		Twist angle: 2.2°
<b>F<sub>2</sub>Mo(C<sub>6</sub>F<sub>5</sub>)<sub>4</sub> (Isomer 1), Tp distorted</b>		( $\alpha$ ) / ( $\beta$ ) / ( $\gamma$ )
	Mo–C <sub>1</sub> 213.3 Mo–C <sub>2</sub> 227.9 Mo–C <sub>3</sub> 209.2 Mo–C <sub>4</sub> 223.0 Mo–F <sub>1</sub> 187.7 Mo–F <sub>2</sub> 190.1	C <sub>1</sub> –Mo–C <sub>2,3,4</sub> 77.2, 135.1, 124.2 C <sub>2</sub> –Mo–C <sub>3</sub> 83.4 C <sub>2</sub> –Mo–C <sub>4</sub> 147.8 C <sub>2</sub> –Mo–C <sub>1</sub> 92.8 C <sub>1</sub> –Mo–F <sub>2,1</sub> 78.7, 97.5 C <sub>4</sub> –Mo–F <sub>1,2</sub> 77.0, 97.5 C <sub>2</sub> –Mo–F <sub>1,2</sub> 76.4, 131.1 C <sub>3</sub> –Mo–F <sub>2,1</sub> 84.6, 116.8 F <sub>1</sub> –Mo–F <sub>2</sub> 149.0
<b>Figure 34.</b> front face (C <sub>1</sub> ,C <sub>2</sub> ,F <sub>1</sub> ) back face (F <sub>2</sub> ,C <sub>3</sub> ,C <sub>4</sub> )		Twist angle: 10.2°

<sup>a</sup> Oct. = octahedral; Tp trigonal prismatic.

From the SHAPE<sup>[23c]</sup> analysis for all the higher members of series F<sub>6-n</sub>M(C<sub>6</sub>X<sub>5</sub>)<sub>n</sub> (M = Mo or W, X = H or F, n = 2 – 4), the following distortion patterns were found: F<sub>4</sub>Mo(C<sub>6</sub>H<sub>5</sub>)<sub>2</sub> as a trigonal prismatic structure lies very close to the C<sub>3v</sub> distortion for a truncated trigonal pyramid and has no significant Bailar distortion (sum of square roots > 4.7), see table 16 and figure 35. F<sub>5</sub>Mo(C<sub>6</sub>H<sub>5</sub>), F<sub>5</sub>W(C<sub>6</sub>H<sub>5</sub>), and F<sub>4</sub>Mo(C<sub>6</sub>F<sub>5</sub>)<sub>2</sub> (isomers 1-3) all have mainly a Bailar distortion ( $\Delta < 9\%$ ) with some little Jahn-Teller type distortion ( $4.2 <$

sum of square roots  $< 4.6$ ) and all lie very close to the same distortive path, see figure 35. On the contrary, *trans*-F<sub>4</sub>Mo(C<sub>6</sub>H<sub>5</sub>)<sub>2</sub> (octahedral), F<sub>3</sub>Mo(C<sub>6</sub>F<sub>5</sub>)<sub>3</sub> and F<sub>2</sub>Mo(C<sub>6</sub>F<sub>5</sub>)<sub>4</sub> are all far away from the pure Bailar path ( $\Delta > 20\%$ ), and the major distortion that they present is most probably a Jahn-Teller type, i.e, the difference in the bond lengths is much more pronounced than in the other complexes.

From all these complexes, F<sub>4</sub>Mo(C<sub>6</sub>H<sub>5</sub>)<sub>2</sub> (Tp, isomer 2) seems to be the closest to the ideal  $D_{3h}$  structure ( $\{S(D_{3h}), S(O_h)\}$  is  $\{0.4, 16.9\}$ ) and F<sub>4</sub>Mo(C<sub>6</sub>F<sub>5</sub>)<sub>2</sub> (isomer 2) is the one with the least deviation from a pure Bailar distortion ( $\Delta = 4.8\%$ ). From the crystallographic evidence of (CH<sub>3</sub>)<sub>4</sub>W(OCH<sub>3</sub>)<sub>2</sub>,<sup>[16]</sup> isomer 2 was the one which crystallized out of the solution, so it might be suggested that a trigonal prismatic structure which has two ligands prefers the arrangement in which the ligands are in the same triangular face, even though it is not the one with the lowest energy requirements. Furthermore, if the ligands are in opposite triangular faces with the highest possible angle ( $\approx 135^\circ$ , which would be the structure with the lowest energy), then it is most probable for the structure to adopt a *trans*-octahedral environment and increase such angle (L-M-L) so that the ligands could have more space. That seems to be the case of *trans*-F<sub>4</sub>Mo(C<sub>6</sub>H<sub>5</sub>)<sub>2</sub>, which is rather octahedral than trigonal prismatic, L-Mo-L  $\approx 142^\circ$ .

**Table 16.** SHAPE<sup>[23c]</sup> analysis for complexes of the type F<sub>6-n</sub>Mo(C<sub>6</sub>X<sub>5</sub>)<sub>n</sub> for n = 2 – 4, and X = H or F.

Complex <sup>a</sup>	S( $D_{3h}$ )	S( $O_h$ )	$\Delta(D_{3h}, O_h)$	$\sqrt{S(D_{3h})} + \sqrt{S(O_h)}$
F <sub>4</sub> Mo(C <sub>6</sub> H <sub>5</sub> ) <sub>2</sub> , Oct.	7.941	5.139	0.220	5.085
F <sub>4</sub> Mo(C <sub>6</sub> H <sub>5</sub> ) <sub>2</sub> , Tp. (Is.2)	0.392	16.892	0.154	4.736
F <sub>4</sub> Mo(C <sub>6</sub> F <sub>5</sub> ) <sub>2</sub> , isomer 1	1.097	12.131	0.093	4.530
F <sub>4</sub> Mo(C <sub>6</sub> F <sub>5</sub> ) <sub>2</sub> , isomer 2	1.596	9.590	0.048	4.360
F <sub>4</sub> Mo(C <sub>6</sub> F <sub>5</sub> ) <sub>2</sub> , isomer 3	0.745	12.353	0.057	4.378
F <sub>3</sub> Mo(C <sub>6</sub> F <sub>5</sub> ) <sub>3</sub> , isomer 1	1.297	15.211	0.221	5.039
F <sub>2</sub> Mo(C <sub>6</sub> F <sub>5</sub> ) <sub>4</sub> , isomer 1	2.532	11.631	0.205	5.002

<sup>a</sup> Oct = octahedral, Tp = trigonal prismatic, Is = Isomer.



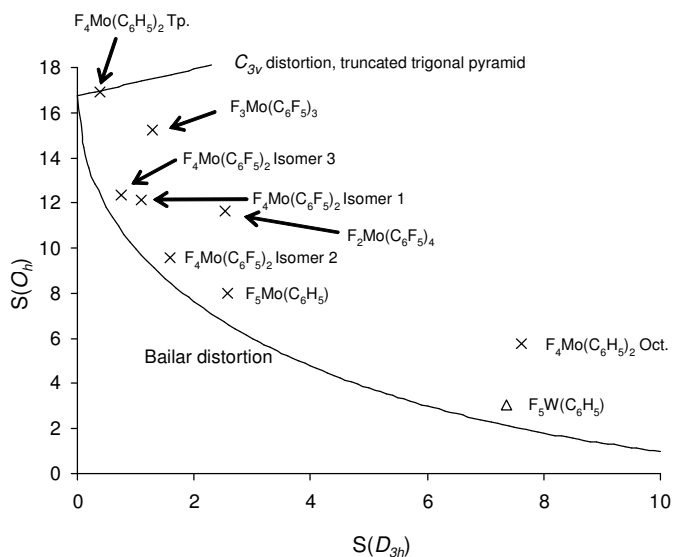


**Figure 35.** Symmetry map for molecules of the type  $F_{6-n}M(C_6X_5)_n$  ( $n = 1 - 4$ ,  $M = Mo$  or  $W$ ,  $X = H$  or  $F$ ), Oct = octahedral, Tp = trigonal prismatic.

#### 2.4 $MoF_6$ and $WF_6$ derivatives with $-SCF_3$ and $-SCH_3$ groups as ligands

While the vast majority of molybdenum and tungsten thiolate complexes are bi- or tridentate chelates with a trigonal prismatic structure (distorted in many cases),<sup>[77-86]</sup> there are only few reports of monomeric monodentate thiolate molybdenum (VI) and tungsten (VI) complexes. The first synthesized complex of this type,  $Cl_5W(SCH_3)$ ,<sup>[87]</sup> was prepared by Boorman, et. al. in 1976. They were not able to isolate any other members of the series  $Cl_{6-n}W(SCH_3)_n$  ( $n \geq 3$ ) because they might have been polymeric species, as it is reported by these authors and complexes of the type  $MoCl_4(SR)_2$  ( $R = -CH_3$  or  $-CH_2CH_3$ ) are believed to be dimeric.<sup>[87]</sup> But no kind of spectroscopical evidence is given for any possible geometry of the central atom.

Furthermore, in 1980 Boorman and O'Dell<sup>[88]</sup> reported the synthesis of  $Cl_5W(SC_6H_5)$ , which decomposes slowly at room temperature over a period of weeks. The authors attribute all unsuccessful attempts with many other thiolate ligands to the instability of the species which either suffer an heterolytic cleavage of the carbon-sulfur bond to generate a carbonium ion which can further abstract chloride to give  $WCl_4 + RCl$ , or to an intermolecular elimination of  $R_2S_2$  like in the case of  $R = -C_6H_5$ . Besides  $^1H$  NMR

and analytical data for the isolated species, they don't discuss any kind of geometry for the central atom.

As it has been suggested in the literature,<sup>[24]</sup> due to the fact that sulfur ligands are fairly weak  $\pi$ -donors, monodentate thiolate complexes should have a structure lying somewhere between an octahedral and trigonal prismatic. In fact,  $[\text{Zr}(\text{SC}(\text{CH}_3)_3)_6]^{2-}$  was resolved better as a trigonal prismatic structure,<sup>[89]</sup> calculations on the hypothetical  $\text{Mo}(\text{SH})_6$  show that it should have a structure with  $C_3$  symmetry just between an octahedron and trigonal prism,<sup>[90]</sup> whereas other hexathiolate complexes<sup>[91-93]</sup> are clearly closer to a trigonal prism.

Based on DFT calculations (discussed in the upcoming section) on molecules of the type  $\text{F}_5\text{MSCX}_3$  with  $M = \text{Mo}$  or  $\text{W}$ , and  $X = \text{H}$  or  $\text{F}$ , a low energy barrier ( $\approx 2 \text{ kcal mol}^{-1}$  for  $M = \text{Mo}$ , and  $\approx 5 \text{ kcal mol}^{-1}$  for  $M = \text{W}$ ) for an octahedral-trigonal prismatic interconversion is obtained. If the energy of this interconversion is that low, the molecules are so fluxional that any possible isolation and characterization of such molecules could result in a structure somehow lying in the path between an  $O_h$  and a  $D_{3h}$ .

Thorough and extensive attempts (like in the case of the aryl derivatives from the previous section) to synthesize molecules of the type  $\text{F}_5\text{MSCF}_3$  with  $M = \text{Mo}$  or  $\text{W}$  were not performed.  $\text{MoF}_6$  and  $\text{WF}_6$  were only reacted with  $\text{Hg}(\text{SCF}_3)_2$  according to reaction scheme (11).



$\text{WF}_6$  and  $\text{Hg}(\text{SCF}_3)_2$  were reacted in  $\text{CH}_2\text{Cl}_2$  at room temperature and even at  $40^\circ\text{C}$  for 1 day and no new signals were detected in the  $^{19}\text{F}$  NMR. No reaction takes place between these two reactants and no further attempts between these two species were carried out.

$\text{MoF}_6$  was reacted with  $\text{Hg}(\text{SCF}_3)_2$  without any solvent. A change in coloration of the mixture suggested a possible reaction. After performing a  $^{19}\text{F}$  NMR of the mixture in  $\text{CCl}_3\text{F}$  the only byproduct detected was  $\text{F}_3\text{CS}-\text{SCF}_3$ .<sup>[71]</sup> No other new signals were seen and no further attempts with these reactants were carried out.

### 2.4.1 DFT calculations: $-\text{SCF}_3$ and $-\text{SCH}_3$ as ligands

Some theoretical calculations on molecules of the type  $\text{F}_5\text{M}(\text{SCX}_3)$  ( $\text{M} = \text{Mo}$  or  $\text{W}$ ,  $\text{X} = \text{H}$  or  $\text{F}$ ) were also performed. All calculated molecules have a ground state which is octahedral (very distorted in some cases) and a transition state (one negative, imaginary frequency) which is trigonal prismatic ( $C_s$  symmetry) (see tables 17 and 18).

From these calculations, in general the molybdenum compounds seem to have a more distorted ground state than the analogous tungsten molecules, in this case being the ground state an octahedral one. In other words, most of the angles in  $\text{F}_5\text{W}(\text{SCH}_3)$  and  $\text{F}_5\text{W}(\text{SCF}_3)$  are much closer to  $90^\circ$  and  $180^\circ$  than in  $\text{F}_5\text{Mo}(\text{SCH}_3)$  and  $\text{F}_5\text{Mo}(\text{SCF}_3)$  respectively. Furthermore, if the distortion these molybdenum complexes present is mainly of the Bailar type, then they would be expected to be closer to a trigonal prismatic structure than the analogous tungsten ones.

The difference in energy between the octahedral ground state and the trigonal prismatic transition state is calculated to be for  $\text{F}_5\text{Mo}(\text{SCH}_3)$  and  $\text{F}_5\text{Mo}(\text{SCF}_3)$   $1.7 \text{ kcal mol}^{-1}$  and  $2.6 \text{ kcal mol}^{-1}$  respectively. The tungsten complexes exhibit a higher energy, namely  $4.5$  and  $5.5 \text{ kcal mol}^{-1}$  for the mercaptan and trifluoromercaptan derivatives respectively. The energies reported here are electronic energies with zero point energy corrections. An extra correction (vibration frequency scaling factor) for the corrected Z.P.E's is needed due to the fact that B3LYP as method and 6-311G(d,p) as basis set were employed.<sup>[94,95]</sup> This scaling factor correction has been taken into account and values are reported with this correction done.

From the energies obtained and from the degree of distortion seen in the angles of these derivatives, it can be said *a priori* that if the complex is “more” Bailar distorted from the octahedral structure, like the molybdenum derivatives, then it is closer to the trigonal prismatic structure, therefore the energy needed for this interconversion would be lower. If that is the case, then  $\text{F}_5\text{Mo}(\text{SCH}_3)$  which has a lower rotation energy barrier than  $\text{F}_5\text{Mo}(\text{SCF}_3)$  would be expected to have a more distorted (Bailar type) octahedral structure. This tendency is also seen in both tungsten cases. That suggests that  $\text{F}_5\text{Mo}(\text{SCF}_3)$  and  $\text{F}_5\text{W}(\text{SCF}_3)$  could be considered “more” octahedral than  $\text{F}_5\text{Mo}(\text{SCH}_3)$

and  $F_5W(SCH_3)$  respectively, since the former have a higher interconversion energy.

**Table 17.** DFT calculations on molecules of the type  $F_5Mo(SCX_3)$ ,  $X = H$  or  $F$ .

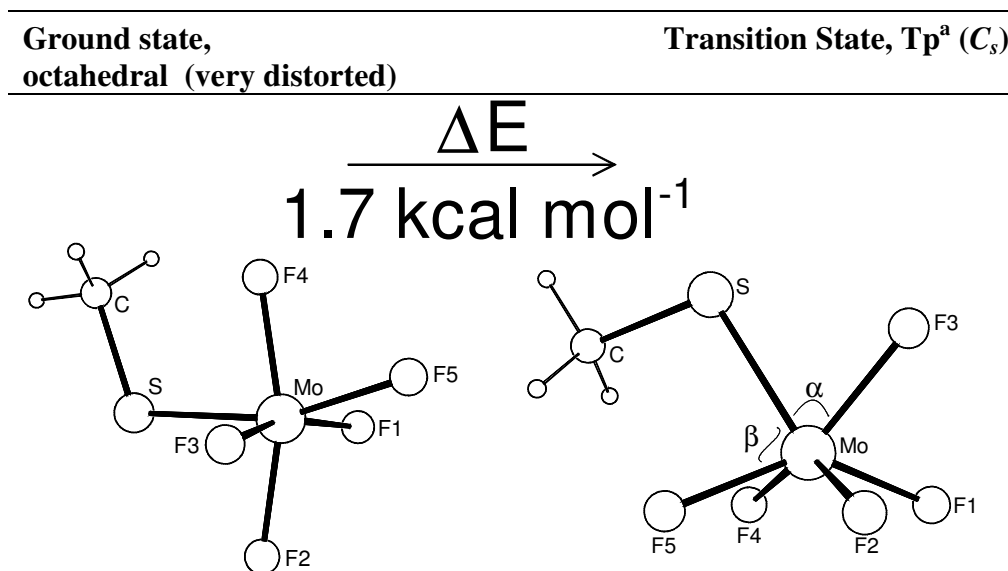


**Figure 36.**  $F_5Mo(SCH_3)$ , Oct. and  $Tp^a$ .

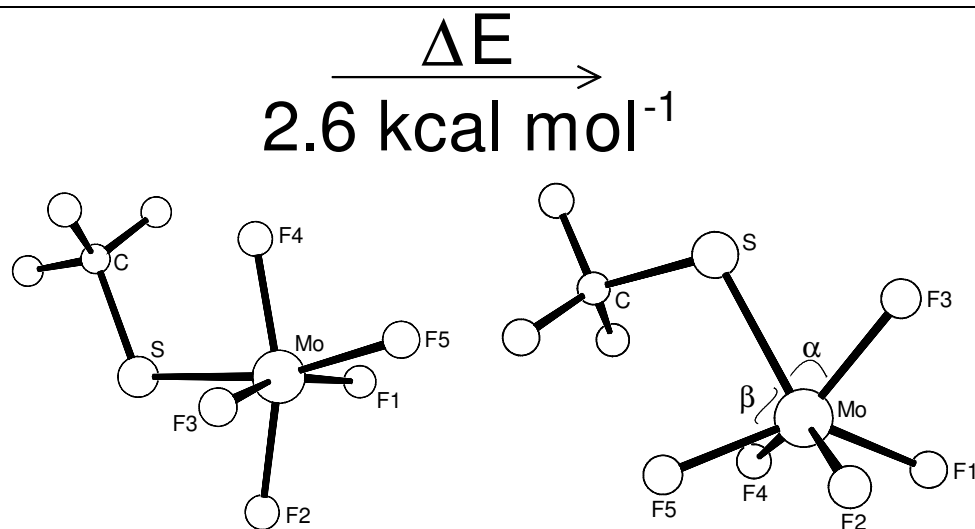
**Selected bond distances (pm)**

Mo-S	234.4	Mo-S	234.0
Mo-F <sub>1</sub>	188.7	Mo-F <sub>1,2</sub>	188.2
Mo-F <sub>2</sub>	187.9	Mo-F <sub>3</sub>	189.9
Mo-F <sub>3</sub>	188.5	Mo-F <sub>4,5</sub>	189.4
Mo-F <sub>4</sub>	189.8	S-C	182.1
Mo-F <sub>5</sub>	189.2		
S-C	181.8		

**Selected angles (°)**

	90° / 180°	(α) / (β) / (γ)
S-Mo-F <sub>1,3</sub>	97.9, 97.8	S-Mo-F <sub>3</sub> 74.0
S-Mo-F <sub>2,4</sub>	81.7, 80.1	S-Mo-F <sub>4,5</sub> 85.7
S-Mo-F <sub>5</sub>	162.0	S-Mo-F <sub>1,2</sub> 128.3
F <sub>1</sub> -Mo-F <sub>2,4</sub>	84.9, 97.5	F <sub>3</sub> -Mo-F <sub>1,2</sub> 82.3
F <sub>1</sub> -Mo-F <sub>3</sub>	160.1	F <sub>3</sub> -Mo-F <sub>4,5</sub> 135.4
F <sub>1</sub> -Mo-F <sub>5</sub>	84.5	F <sub>4</sub> -Mo-F <sub>1,2</sub> 80.1 138.6
F <sub>2</sub> -Mo-F <sub>4</sub>	161.9	F <sub>4</sub> -Mo-F <sub>5</sub> 79.9
F <sub>3</sub> -Mo-F <sub>2,4</sub>	85.0, 97.4	F <sub>1</sub> -Mo-F <sub>2</sub> 91.7
F <sub>3</sub> -Mo-F <sub>5</sub>	84.7	S-Mo-C 104.9
F <sub>5</sub> -Mo-F <sub>2,4</sub>	116.3, 81.8	
S-Mo-C	111.4	Twist angle: 0°

Continuation table 17.

Figure 37. F<sub>5</sub>Mo(SCF<sub>3</sub>), Oct. and Tp.<sup>a</sup>

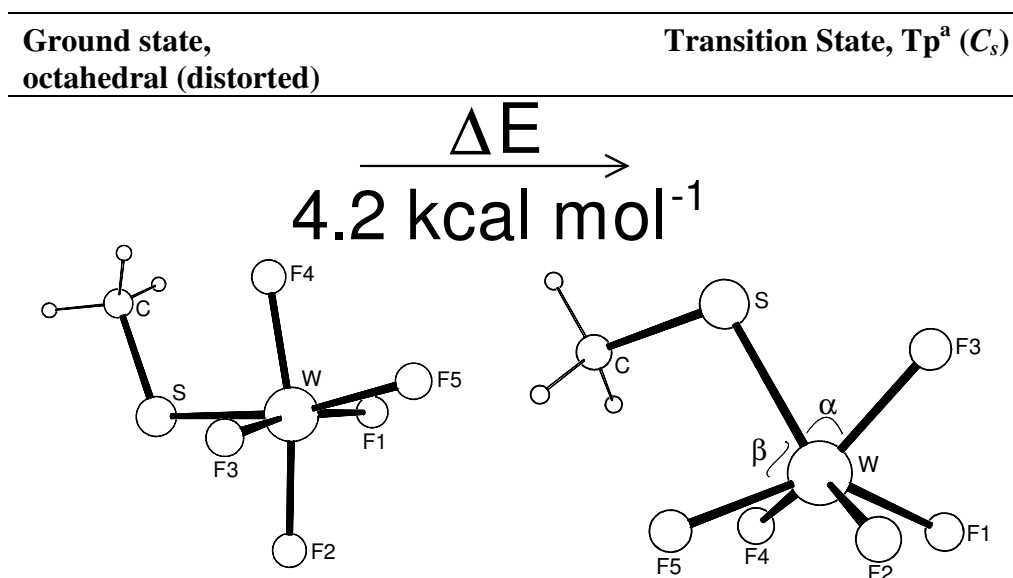
## Selected bond distances (pm)

Mo-S	238.1	Mo-S	237.6
Mo-F <sub>1</sub>	187.7	Mo-F <sub>1,2</sub>	187.5
Mo-F <sub>2</sub>	187.8	Mo-F <sub>3</sub>	189.8
Mo-F <sub>3</sub>	187.6	Mo-F <sub>4,5</sub>	187.9
Mo-F <sub>4</sub>	187.6	S-C	186.1
Mo-F <sub>5</sub>	188.5		
S-C	185.7		

## Selected angles (°)

	90° / 180°	( $\alpha$ ) / ( $\beta$ ) / ( $\gamma$ )
S-Mo-F <sub>1,3</sub>	97.6, 97.4	S-Mo-F <sub>3</sub> 72.0
S-Mo-F <sub>2,4</sub>	78.8, 81.5	S-Mo-F <sub>4,5</sub> 87.2
S-Mo-F <sub>5</sub>	165.8	S-Mo-F <sub>1,2</sub> 128.6
F <sub>1</sub> -Mo-F <sub>2,4</sub>	84.7, 97.7	F <sub>3</sub> -Mo-F <sub>1,2</sub> 82.8
F <sub>1</sub> -Mo-F <sub>3</sub>	159.8	F <sub>3</sub> -Mo-F <sub>4,5</sub> 135.1
F <sub>1</sub> -Mo-F <sub>5</sub>	84.4	F <sub>4</sub> -Mo-F <sub>1,2</sub> 80.1 137.9
F <sub>2</sub> -Mo-F <sub>4</sub>	160.4	F <sub>4</sub> -Mo-F <sub>5</sub> 80.7
F <sub>3</sub> -Mo-F <sub>2,4</sub>	85.0, 97.9	F <sub>1</sub> -Mo-F <sub>2</sub> 89.8
F <sub>3</sub> -Mo-F <sub>5</sub>	84.5	S-Mo-C 109.23
F <sub>5</sub> -Mo-F <sub>2,4</sub>	115.4, 84.2	
S-Mo-C	111.1	Twist angle: 0°

<sup>a</sup> Oct. = octahedral, Tp = trigonal prismatic.

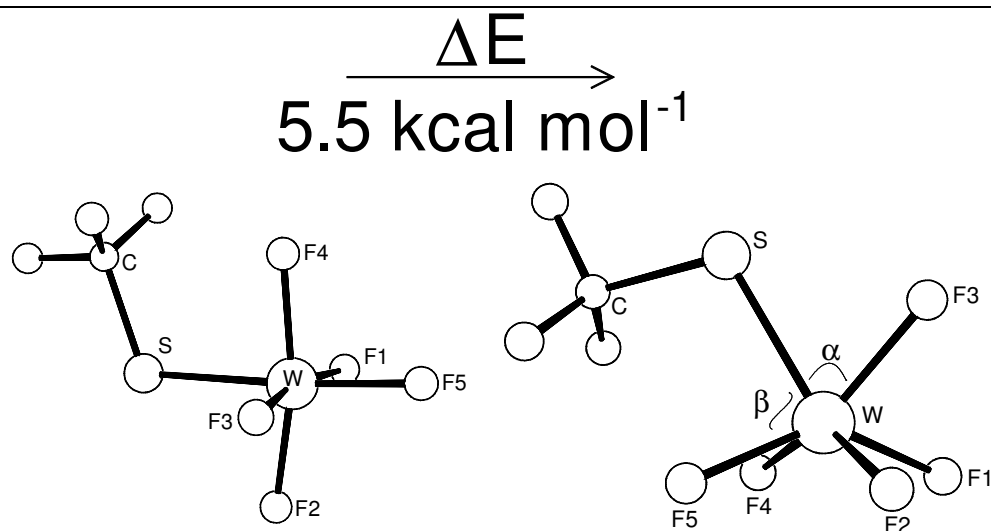
**Table 18.** DFT calculations on molecules of the type  $F_5W(SCX_3)$ ,  $X = H$  or  $F$ .**Figure 38.**  $F_5W(SCH_3)$ , Oct. and  $Tp^a$ **Selected bond distances (pm)**

W-S	235.3	W-S	235.3
W-F <sub>1</sub>	189.6	W-F <sub>1,2</sub>	189.2
W-F <sub>2</sub>	188.0	W-F <sub>3</sub>	190.6
W-F <sub>3</sub>	189.3	W-F <sub>4,5</sub>	189.9
W-F <sub>4</sub>	189.7	S-C	183.0
W-F <sub>5</sub>	190.5		
S-C	182.9		

**Selected angles (°)**

	90° / 180°	( $\alpha$ ) / ( $\beta$ ) / ( $\gamma$ )
S-W-F <sub>1,3</sub>	95.7, 97.1	S-W-F <sub>3</sub> 74.4
S-W-F <sub>2,4</sub>	85.4, 83.4	S-W-F <sub>4,5</sub> 86.7
S-W-F <sub>5</sub>	167.9	S-W-F <sub>1,2</sub> 128.5
F <sub>1</sub> -W-F <sub>2,4</sub>	87.0, 95.3	F <sub>3</sub> -W-F <sub>1,2</sub> 82.0
F <sub>1</sub> -W-F <sub>3</sub>	164.9	F <sub>3</sub> -W-F <sub>4,5</sub> 136.0
F <sub>1</sub> -W-F <sub>5</sub>	84.0	F <sub>4</sub> -W-F <sub>1,2</sub> 79.5 137.7
F <sub>2</sub> -W-F <sub>4</sub>	168.7	F <sub>4</sub> -W-F <sub>5</sub> 80.2
F <sub>3</sub> -W-F <sub>2,4</sub>	86.3, 93.9	F <sub>1</sub> -W-F <sub>2</sub> 91.2
F <sub>3</sub> -W-F <sub>5</sub>	85.1	S-W-C 104.7
F <sub>5</sub> -W-F <sub>2,4</sub>	106.7, 84.6	
S-W-C	111.6	Twist angle: 0°

Continuation table 18.

Figure 39. F<sub>5</sub>W(SCF<sub>3</sub>), Oct. and Tp.<sup>a</sup>**Selected bond distances (pm)**

W-S	239.6	W-S	239.2
W-F <sub>1</sub>	188.7	W-F <sub>1,2</sub>	188.5
W-F <sub>2</sub>	187.6	W-F <sub>3</sub>	190.4
W-F <sub>3</sub>	188.6	W-F <sub>4,5</sub>	188.5
W-F <sub>4</sub>	187.3	S-C	185.9
W-F <sub>5</sub>	189.7		
S-C	185.5		

**Selected angles (°)**

	90° / 180°	(α) / (β) / (γ)
S-W-F <sub>1,3</sub>	95.7, 95.5	S-W-F <sub>3</sub> 72.3
S-W-F <sub>2,4</sub>	82.0, 85.9	S-W-F <sub>4,5</sub> 87.2
S-W-F <sub>5</sub>	176.0	S-W-F <sub>1,2</sub> 128.9
F <sub>1</sub> -W-F <sub>2,4</sub>	87.8, 93.5	F <sub>3</sub> -W-F <sub>1,2</sub> 82.6
F <sub>1</sub> -W-F <sub>3</sub>	167.4	F <sub>3</sub> -W-F <sub>4,5</sub> 135.4
F <sub>1</sub> -W-F <sub>5</sub>	84.5	F <sub>4</sub> -W-F <sub>1,2</sub> 79.6
F <sub>2</sub> -W-F <sub>4</sub>	167.9	F <sub>4</sub> -W-F <sub>5</sub> 81.1
F <sub>3</sub> -W-F <sub>2,4</sub>	88.0, 93.1	F <sub>1</sub> -W-F <sub>2</sub> 89.3
F <sub>3</sub> -W-F <sub>5</sub>	84.7	S-W-C 108.8
F <sub>5</sub> -W-F <sub>2,4</sub>	101.9, 90.7	
S-W-C	109.2	Twist angle: 0°

<sup>a</sup> Oct. = octahedral, Tp = trigonal prismatic.

In fact, a SHAPE<sup>[23c]</sup> analysis on all four octahedral ground states and trigonal prismatic transition states (Table 19) confirms all these previous assumptions:

1. All four ground state molecules are octahedrons with a significant Jahn-Teller- and Bailar type distortions.
2. The tungsten complexes are more octahedral than the corresponding molybdenum ones, i.e. the later are more trigonal prismatic.
3. The –SCF<sub>3</sub> complexes are more octahedral than the –SCH<sub>3</sub> ones, i.e. the later are more distorted towards a trigonal prism.

All trigonal prismatic transition states have a  $C_{3v}$  distortion type, see figure 40, exactly like it was the case for the molecules of the type  $F_5MCX_3$ . In this transition state the molybdenum complexes are less distorted from the ideal  $D_{3h}$  structure than the tungsten ones. Furthermore,  $F_5Mo(SCH_3)$  is the most distorted octahedral structure and its transition state is the less distorted trigonal prism. It also happens to have the lowest energy difference between the two states.

So indeed, the higher the energy of the octahedral-trigonal prismatic rearrangement, the more octahedral the ground state is and the less trigonal prismatic the transition state would be.

**Table 19.** SHAPE<sup>[23c]</sup> analysis for complexes of the type  $F_5M(SCX_3)$  for  $M = Mo$  or  $W$ , and  $X = H$  or  $F$ .

Complex <sup>a</sup>	$S(D_{3h})$	$S(O_h)$	$\Delta(D_{3h}, O_h)$	$\sqrt{S(D_{3h})} + \sqrt{S(O_h)}$
$F_5Mo(SCH_3)$ Oct. (Gs)	9.669	3.346	0.187	4.939
$F_5Mo(SCF_3)$ Oct. (Gs)	9.942	3.337	0.200	4.980
$F_5Mo(SCH_3)$ Tp. (Ts)	0.784	17.200	0.225	5.033
$F_5Mo(SCF_3)$ Tp. (Ts)	0.964	17.306	0.251	5.142



Continuation table 19.

$F_5W(SCH_3)$ Oct. (Gs)	11.273	1.971	0.147	4.761
$F_5W(SCF_3)$ Oct. (Gs)	13.105	1.608	0.181	4.888
$F_5W(SCH_3)$ Tp. (Ts)	0.864	17.248	0.237	5.083
$F_5W(SCF_3)$ Tp. (Ts)	1.027	17.343	0.260	5.178

<sup>a</sup> Oct.= octahedral, Tp = trigonal prismatic, Gs = ground state, Ts = transition state.

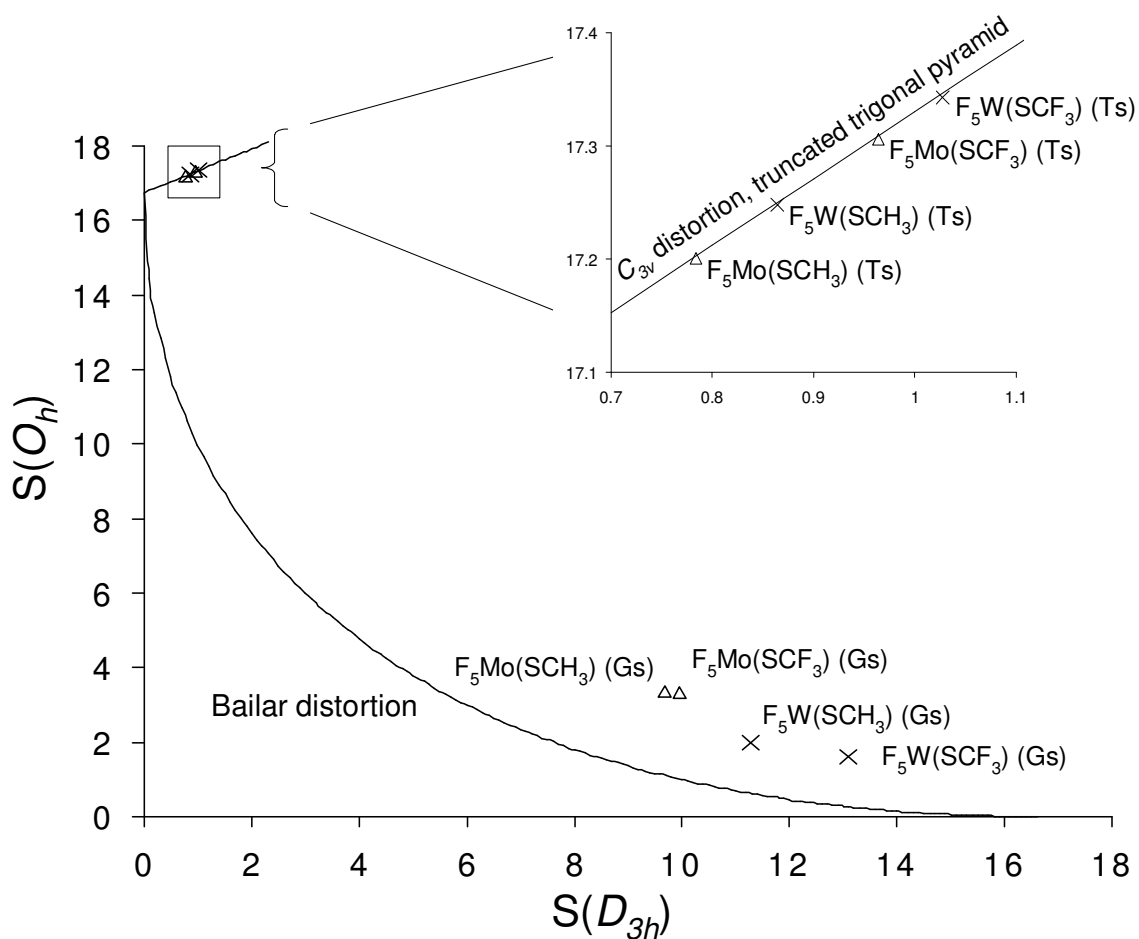


**Figure 40.** Symmetry map for molecules of the type  $F_5M(SCX_3)$  ( $M = Mo$  or  $W$ ,  $X = H$  or  $F$ ), Gs = ground state, Ts = transition state.